VISCOSITY OF THE SEPARATED ISOTOPES OF LITHIUM

Thesis for the Degree of M. S.
MICHIGAN STATE UNIVERSITY
Charles M. Randall
1962

ABSTRACT

VISCOSITY OF THE SEPARATED ISOTOPES
OF MOLTEN LITHIUM

by Charles M. Randall

In previous work at Michigan State University the viscosity of molten Li^6 and Li^7 was determined as a function of temperature. The dependence of viscosity on temperature followed an exponential law, in conformity with the finding for most liquids. The dependence on isotopic mass, however, was much stronger than predicted by simple theories. In the present work, a careful repetition of the experiment failed to give results significantly different from those obtained earlier. Hence the theoretical basis was re-examined. Fundamental theories of the liquid state are not sufficiently well established to permit meaningful predictions on the effect of isotopic mass, but some semiempirical laws are available that predict variation as the square root of the mass. Earlier dimensional-analysis arguments had indicated this same type of dependence. A complete treatment, however, shows that the square-root factor must be multiplied by a complementary function depending on the mass through quantum effects. Hence, a strong dependence on mass is not inconsistent with the results of dimensional analysis. In fact, in the only other unequivocal study on the effect of isotopic mass (with liquid hydrogen and deuterium) a similar anomaly is observed. It appears that further progress will depend on having many more measurements of the viscosity of liquids as a function not merely of temperature and pressure, but also of isotopic mass.

VISCOSITY OF THE SEPARATED ISOTOPES OF LITHIUM

By

Charles M. Randall

A THESIS

Submitted to
Michigan State University
in partial fulfillment of the requirements
for the degree of

MASTER OF SCIENCE

Department of Physics and Astronomy

1962

ACKNOWLEDGMENTS

It is my pleasure to express my sincere appreciation to Doctor D. J. Montgomery who suggested the problem and who has guided the work and has been a source of encouragement as it has progressed. His wide knowledge, patience, and the unstinting contribution of his time are all gratefully acknowledged.

Though I have never personally meet Doctor N. T. Ban I would like to express my appreciation for the careful work he has done on the experimental method. His carefully-kept records have made my work much easier.

Mr. Frank Taylor has taken most of the data for Li^6 and done many of the calculations for both isotopes. His patient and careful work is certainly appreciated.

I would like to express my thanks also to: Mr. Richard Haire of the Department of Chemistry for his assistance in the chemical analysis of some of the samples, and Mr. Jerry Tomecek who has helped with the data processing and drafting.

Major financial support has come from the United States Atomic Energy Commission. More recent support has come from the National Science Foundation through a Cooperative Graduate Fellowship. To these sources of support I am grateful.

The most important source of encouragement during this work has been my wife. In addition to the encouragement she has continually offered, she has taken time from her already crowded schedule to help with the material production of this thesis through typing of rough drafts and lettering the captions on the figures. For this help I am extremely grateful.

****

TABLE OF CONTENTS

LIST OF TABLES

LIST OF FIGURES

LIST OF APPENDICES

CHAPTER I

INTRODUCTION

When the existence of stable isotopes was established nearly a half century ago, it was immediately realized that isotopic mass could be utilized in studies of matter in the aggregate (1). Unfortunately the enrichments necessary to get meaningful results were not available until about 1945. Then high-current mass spectrometers left over from war-time atomic energy projects found utilization; the United States Atomic Energy Commission in particular instituting a program of supplying separated stable isotopes of most of the elements.

Among the properties of liquids, viscosity appears to be a parameter which would depend on the isotopic mass in some strong but non-trivial manner, for viscosity must be controlled both by the frequency of atomic vibration (depending on the square root of isotopic mass), and by the amplitude of atomic vibration (determined by quantum phenomena affected by isotopic mass).

For simplicity of interpretation, a monatomic liquid would be best. For a large relative mass difference an element of low atomic number must be chosen. Helium (He^3, He^4) forms a liquid with very special properties, and hydrogen (H^1, H^2) forms a molecular liquid; but both of these condense only at inconveniently low temperatures. Lithium (Li^6, Li^7) forms a monatomic liquid at a convenient temperature (melting point, $\sim 180^{\circ}C$). In addition the separated isotopes of lithium are available in gram quantities at reasonable prices. The next several elements in the periodic table are unsuitable for one reason or another.

Because of its high specific heat, lithium has been suggested as a coolant for nuclear reactors both fission and fusion. Hence the viscosity of the separated isotopes has considerable technological interest.

Values for the viscosity of natural lithium (7.4% Li^6, 92.6% Li^7) have been reported, but the values remain uncorroborated (2). The results, then, from any investigation on the viscosity of the isotopes of lithium would have technological as well as scientific interest.

Such measurements on the separated isotopes of lithium were made at Michigan State University by Dr. N. T. Ban (3). The behavior of each isotope singly was consistent with the usual laws found for the temperature dependence of viscosity, but the comparison between the isotopes showed that the dependence on isotopic mass was much stronger than had been expected. The theory of liquid metals is not highly developed, and hence it is uncertain just how reliable are the theoretical predictions. Furthermore, the experiment is difficult, in view of the small amounts of lithium available and its high chemical reactivity.

The dependence on isotopic mass is a critical test of any fundamental theory of viscosity, and it is important to assess carefully the reliability of the experimental results on lithium, as well as the validity of the theoretical deductions. The purpose of the present work is to repeat some of the measurements made by Ban, searching for possible sources of error and evaluating their magnitude; and to re-examine some of the theoretical arguments put forth, to see if experimental results are truly discordant with theory.

CHAPTER II

EXPERIMENTAL METHOD

A. Choice of Method

There are a number of experimental methods available to measure viscosity, each having its characteristic advantages and disadvantages. These methods are explained in detail in several books (4, 5). Common methods are: flow through a capillary, flow through an orfice, rise of a bubble in the fluid, descent of an object in the fluid, and drag between rotating concentric cylinders or cones. Because molten lithium is extremely reactive (6) and the separated isotopes are available only in limited quantities none of the conventional methods are useful. In view of these considerations Ban adopted a method consisting of measuring the damping of the free oscillations of a torsion pendulum containing a spherical cavity filled with the liquid, as originally developed by Helmholtz and Piotrowski in 1816. The damping is related to the viscosity by a mathematical formula allowing an absolute determination of the viscosity. Although original workers had difficulty with their mathematical analysis and experimental technique, the method has been improved through the years (7, 8) so that it will give reliable results, In particular Andrade and Chiong (9) have developed a method of simplifying the calculations.

In the analysis, the fluid is assumed to move slowly in concentric spherical shells around a vertical axis, with no vertical component of motion. The major damping effect on the pendulum is assumed to be due to the viscous drag of the fluid at the liquid-sphere interface. From the hydrodynamical equations of motion, the damping force is shown to be proportional to the time rate of change of the angular displacement θ about a vertical axis. The proportionality constant L, is a complex

number; however, it is still possible to describe the motion with the familiar second-order differential equation of the damped free harmonic oscillator:

$$I\ddot{\theta} + L\dot{\theta} + M\theta = 0 \tag{1}$$

Here I is the moment of inertia of the oscillating system, and $M\theta$ is the restoring torque.

When this equation with the damping force as determined by the hydrodynamical equation is solved, the following expression for the coefficient of viscosity η is obtained in terms of measured quantities:

$$\eta = \frac{a^2R^2\pi\rho}{4(2-q)^2T} \left[1 - (1 - u)^{\frac{1}{2}}\right]^{\frac{1}{2}},$$

where

$$u \equiv \frac{3(2-q)I\delta}{2\pi^2a^2\rho R^5} \left[\frac{T^2}{T_0^2} + 1\right], \tag{2}$$

$$q \equiv \frac{gR-1}{(gR-1)^2 + (hR)^2},$$

$$a = 1 - \delta/4\pi + \delta^2/32\pi^2,$$

$$g = a(\pi\rho/T\eta)^{\frac{1}{2}},$$

$$h = (\pi\rho/T\eta)(1 + \delta/4\pi + \delta^2/32\pi^2).$$

The experimentally-measured quantities are:

I = moment of inertia of oscillating system

R = inside radius of sphere

ρ = density of fluid

δ = logarithmic decrement of pendulum

T = period of pendulum with damping present

T_0 = period of pendulum with damping absent

The experimental set-up consists of a torsion pendulum oscillating in a vacuum, so that the major damping force is the viscous drag of the molten lithium. With the amounts of lithium available, this damping force is small, and consequently introduces special complications in its measurement. We now review the experimental apparatus in some detail, and see how each of the above parameters is measured. Later each type of measurement will be re-examined in an attempt to find possible sources of errors.

B. Design of Apparatus

The torsion pendulum is similar to the one described by Andrade and Chiong (9). The present apparatus was designed and constructed under the supervision of N. T. Ban. The details of the torsion pendulum are shown in Figure 1. The head, A, which is the top support for the bifilar tungsten suspension, passes through the top of the vacuum chamber, B. It is sealed in place by two O-rings, and can be rotated about a vertical axis to bring it to any desired location, or to start the pendulum oscillating. The top of the vacuum chamber can be leveled with three screws. The entire pendulum is enclosed in a vacuum chamber, H, connected to a conventional vacuum system consisting of a diffusion pump and a mechanical fore pump, along with the associated cold trap, valves, and gauges. Brass bellows have been installed part way down the vacuum enclosure to allow the lower part of the vacuum enclosure to be oriented for proper clearance of the pendulum inside. Near the bottom of the tubular part of the vacuum enclosure two windows are cemented 90° apart about a vertical axis. The bottom of the tungsten suspension is fastened to the oscillating system slightly above the level of these windows. At the level of the windows a mirror is fastened to the oscillating system so that the oscillations of the pendulum may be

Scale: 1/4

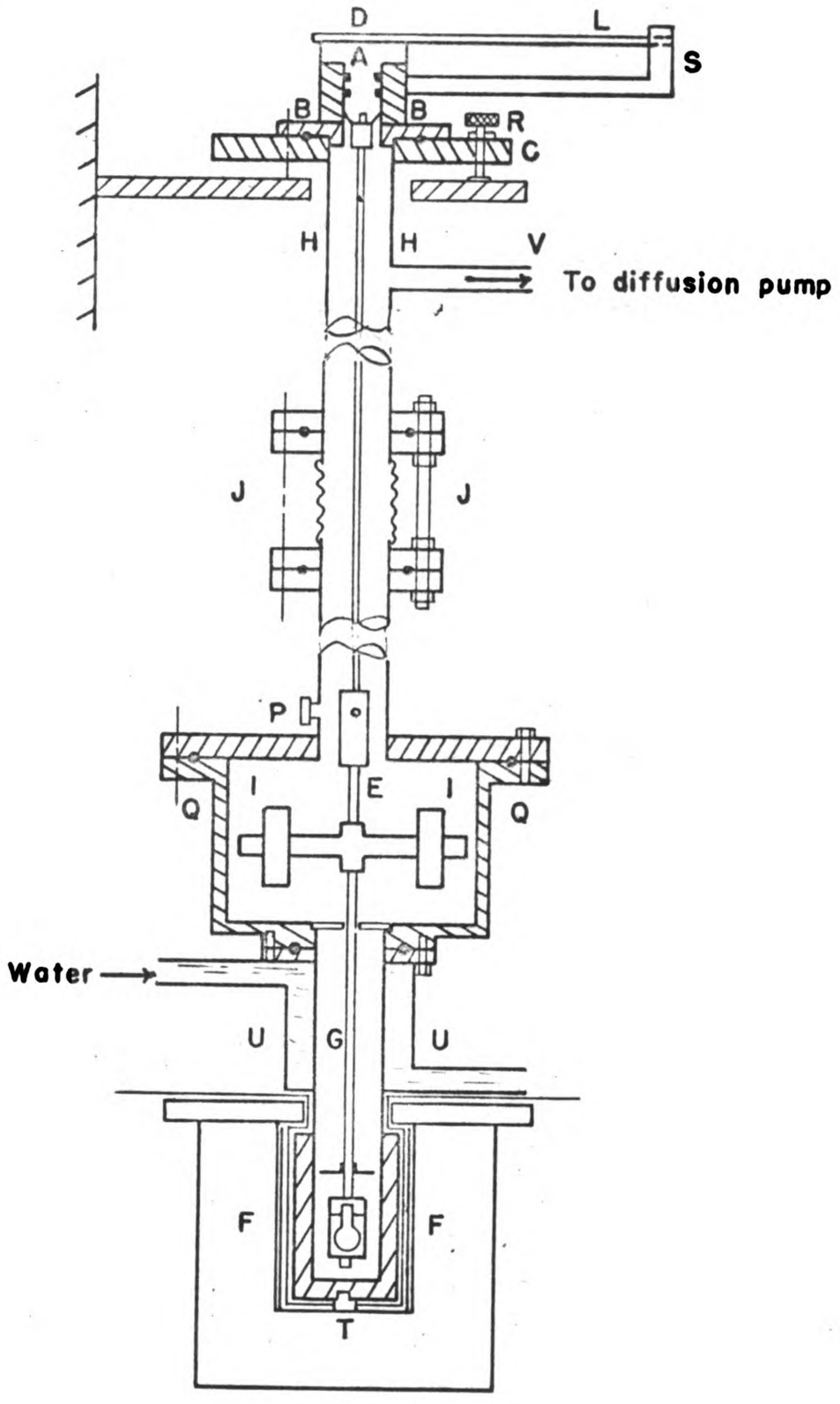

FIGURE 1

GENERAL VIEW OF APPARATUS

observed by means of an optical lever. Below the mirror are two masses, I, whose position may be adjusted to vary the period of the pendulum. A rubber vacuum hose is attached to a copper tube soldered into the vacuum enclosure, Q, and then clamped off with pinch clamps. Thermocouples may be inserted in the vacuum chamber through this hose, which is then filled with vacuum grease and squeezed tight with two or three pinch clamps. Below the inertia arms, with their movable masses, the sphere is suspended from a long stainless-steel tube, G, which has a number of holes drilled in it to increase the resistance of the thermal path from the sphere. The chamber wall around the sphere is a hollow cylinder of copper attached by a short piece of stainless-steel tubing to the water jacket, U. A copper-constantan thermocouple is installed in the bottom of the copper block. This thermocouple is used to measure the temperature of the sphere, and also to actuate the recorder-controller for the temperature of the furnace, F. A detailed view of the sphere is shown in Figure 2. The sphere is made of ferritic stainless steel (Type 446), which is supposed to be especially resistant to corrosion by molten lithium (6). Specific construction details are given in Ban's thesis. A photograph of the experimental area is shown in Figure 3.

C. Observation of Oscillations

The measurements on the pendulum oscillations must yield the following data: the period T when the lithium is liquid, and the period T_0 when the lithium is solid, and the logarithmic decrement δ in both cases. The observation system is shown schematically in Figure 4, and is in principle identical to the system used by Ban. However, the auxiliary equipment has been almost completely rebuilt to increase its reliability and convenience. The Sanborn Millivac recorder used by Ban is no

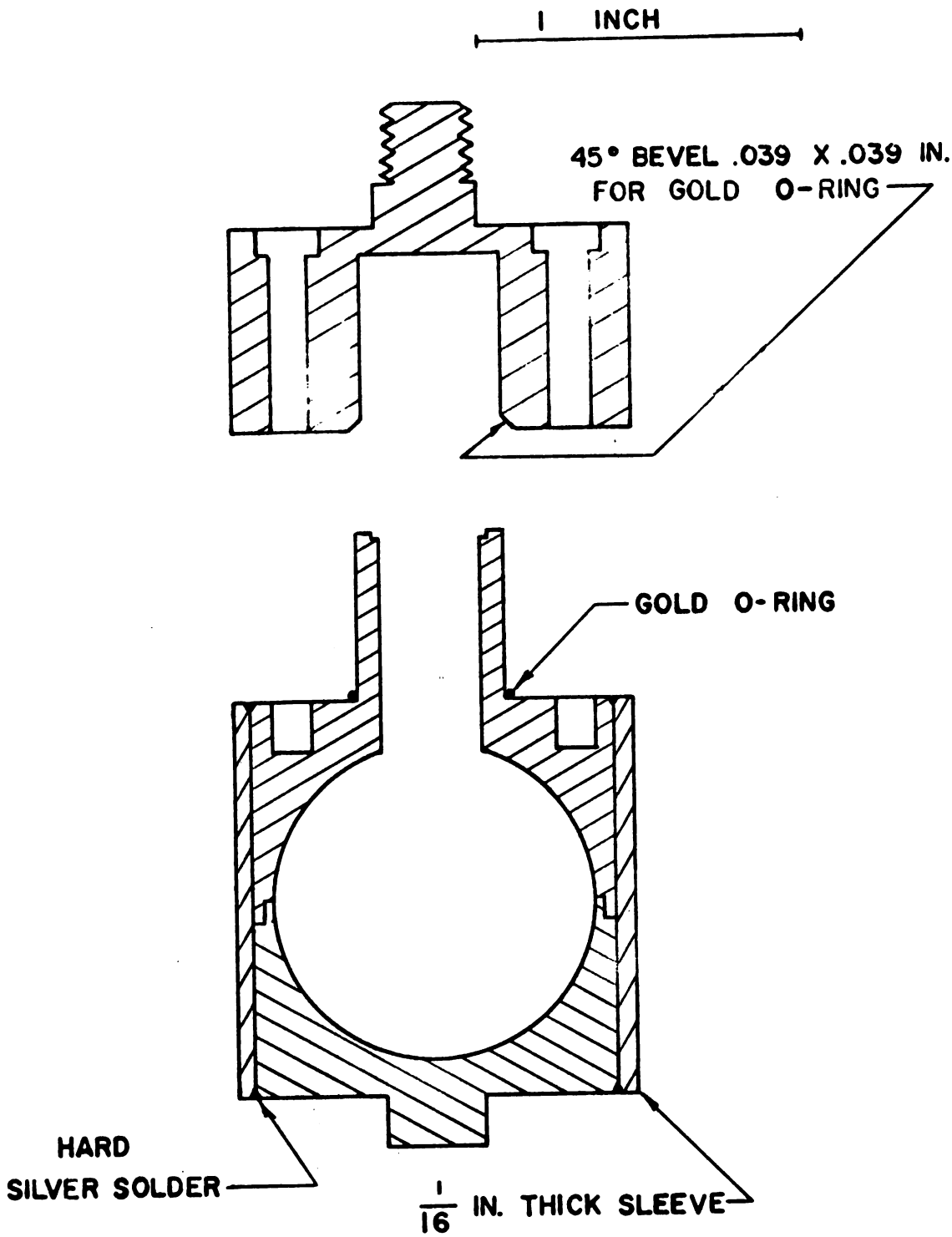

FIGURE 2

LI SAMPLE HOLDER

MATERIAL: STAINLESS STEEL TYPE 446

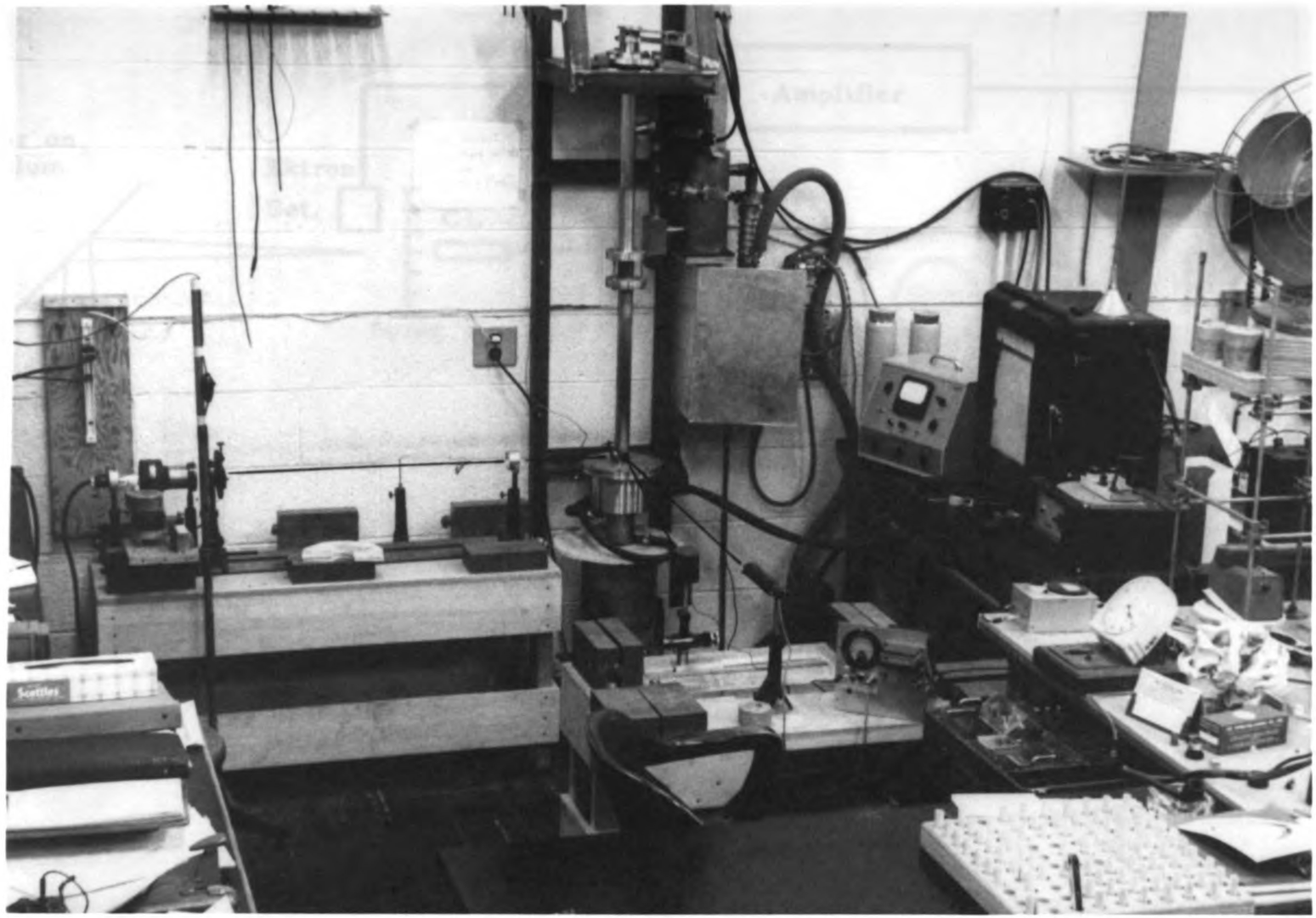

Figure 3 - General view of experimental arrangement. At the far left is the light source, which projects the light beam to the right until it reaches the window in the vacuum chamber hanging vertically from a steel framework bolted to the wall. To the right appear the vacuum gauge and the Speedomax controller for the furnace. The photosensitive cells and recording apparatus, are in the center and right foreground.

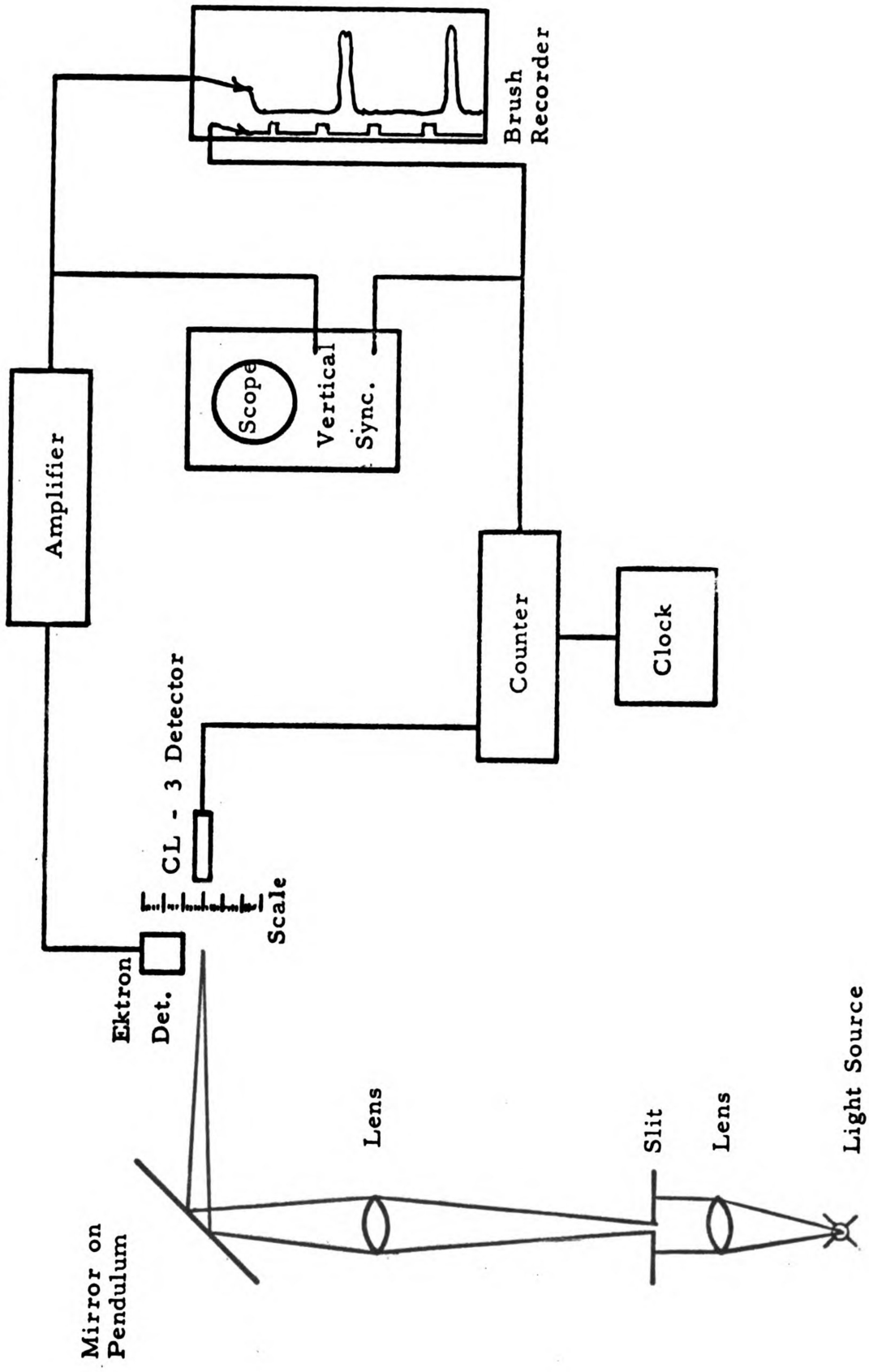

Figure 4 - Schematic view of system for observing oscillations.

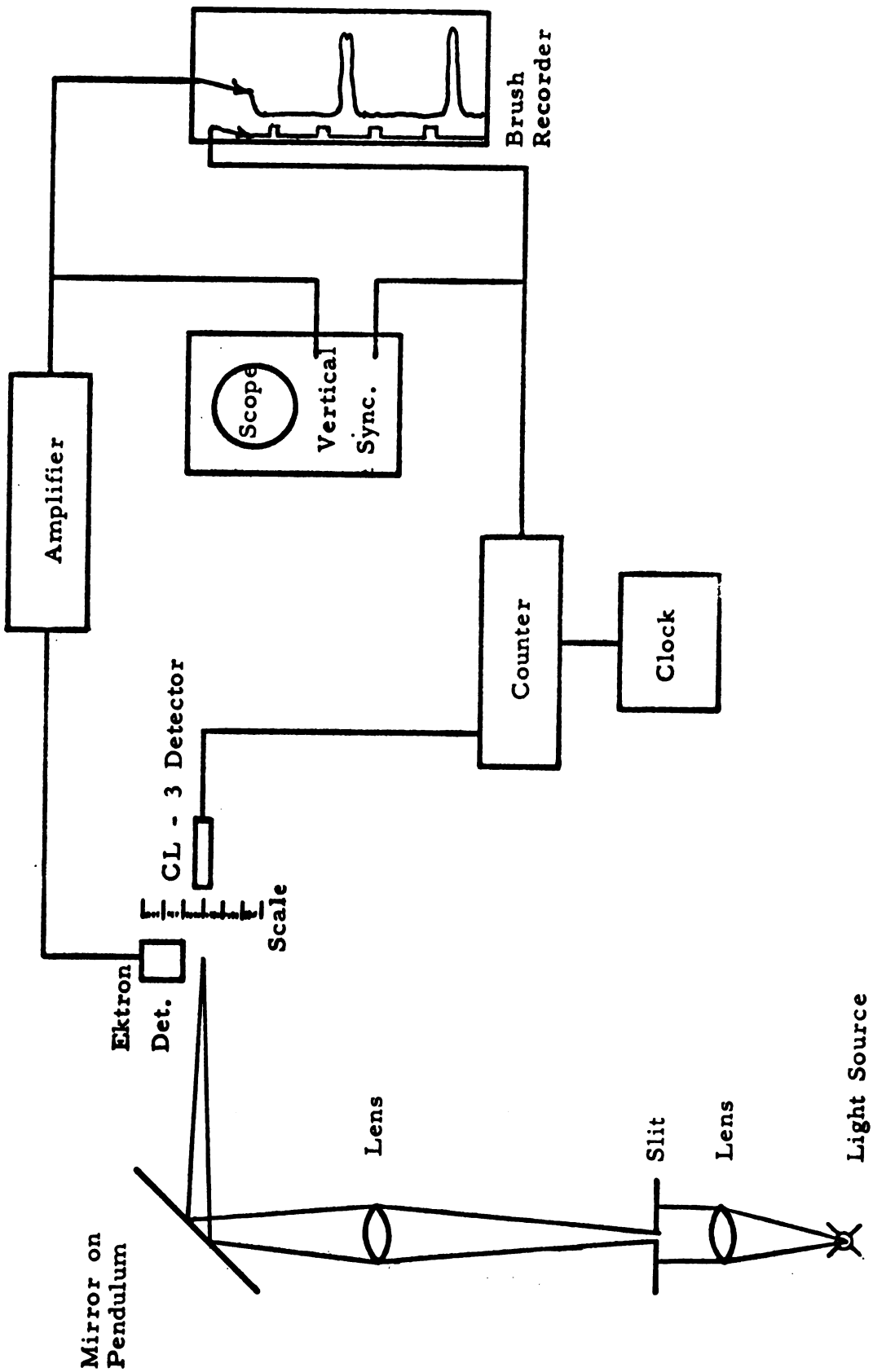

Figure 4 - Schematic view of system for observing oscillations.

longer available, and the apparatus has been modified to use a Brush two-channel recorder available from another project. The oscilloscope and the recorder display the same information. The oscilloscope allows adjustment of the equipment without wasting chart paper, and the recorder allows a permanent record to be made when data runs are underway.

The light source consists of a 10-watt concentrated arc lamp at the focal point of a converging lens. The resulting parallel beam of light is passed through a slit, an image of which is focussed on the window of the photocell used to measure the logarithmic decrement.

One detector is a cadmium-selenide photoresistor (Clairex CL-3) placed about halfway between the maximum excursions of the light beam. This cell is connected to the counter circuit shown in Figure 5. The circuit uses the 2D21 thyratron as a grid-controlled rectifier. Passage of the light beam over the face of the photocell causes its resistance to change. The resulting change in current creates a positive voltage pulse which overcomes the negative bias on the grid of the 2D21 and causes the tube to conduct. The RC-network containing the relay coil, the counter coil, the resistor, R_1, and the capacitor, C_1, is designed to keep the tube in the conducting state long enough for the counter to be positively actuated and the relay firmly closed. The connector marked "to Scope Sweep" provides a pulse to trigger the sweep of the oscilloscope. The relay controls a second pen on the Brush recorder, and through appropriate latching relays and switches actuates a self-starting electric clock, which is started by one pulse and turned off by a succeeding one. In this way the periods T and T_0 can be determined by allowing one pulse to start the clock and a later pulse to turn it off while the counter registers the number of intervening pulses representing oscillations of the pendulum.

The logarithmic decrement is measured by a lead-sulphide photoresistor (Kodak Ektron detector), having a sensitive area 0.02 mm by

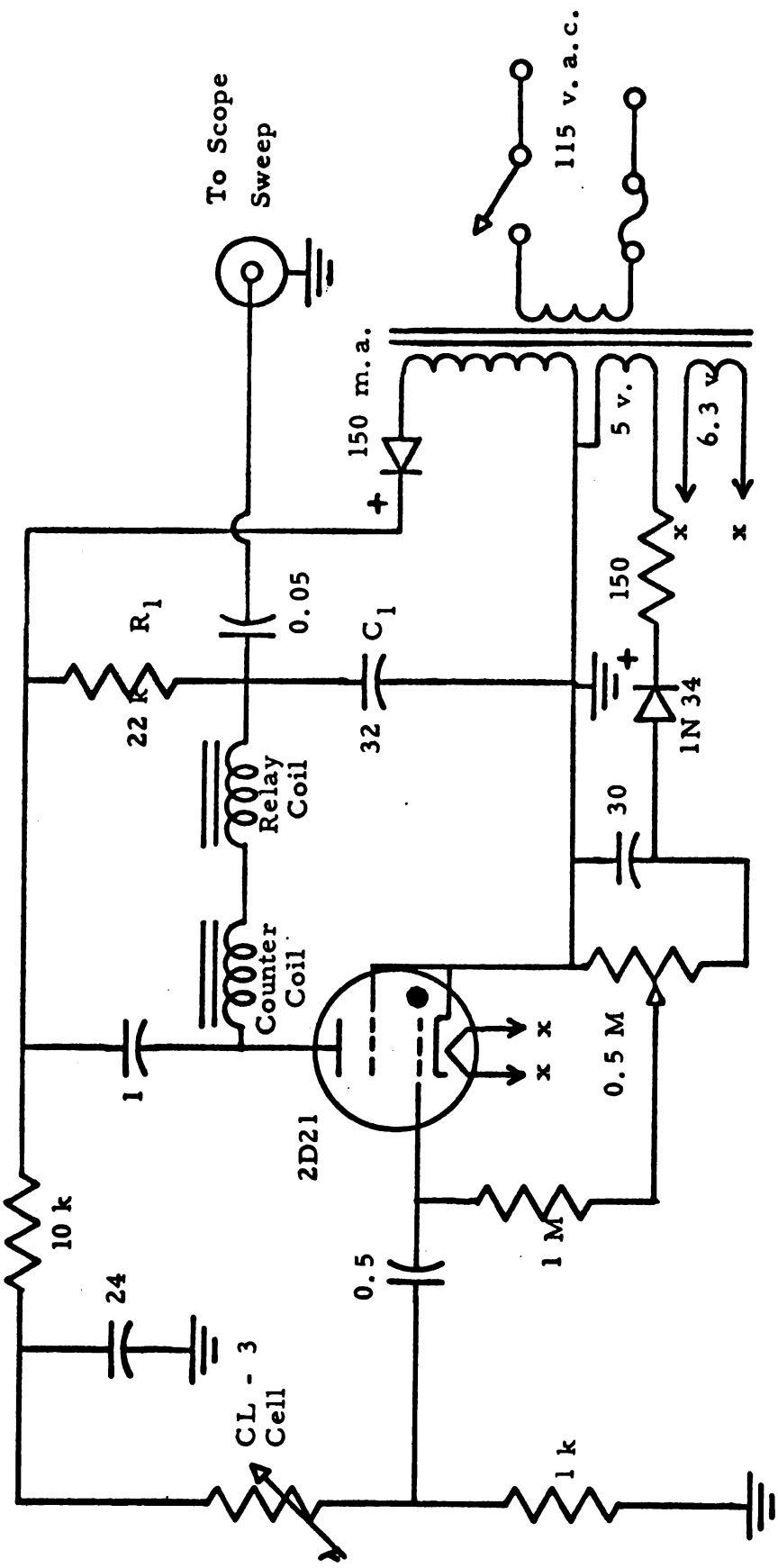

Figure 5
Counter Circuit

2 mm. It is placed in a circuit, shown in Figure 6, which contains a mercury battery serving as a current source for the detector, and a two-stage voltage amplifier with a long time constant. The output of this amplifier is fed to the vertical input of the oscilloscope and to the amplifier of the Brush recorder.

The Ektron detector is mounted on a screw carriage to permit positioning of the detector to within 0.01 mm over a range of about 5 cm. This screw carriage is in turn fastened to a sliding carriage having a vernier scale which likewise may be read to 0.01 mm. This sliding carriage has a travel of about 35 cm, and permits a coarse adjustment of the position over a wide range. The detector is placed near the point of maximum excursion of the oscillating light beam. When the light beam goes beyond the detector, the oscilloscope and the recorder reveal a pulse with two peaks (or even two separate pulses when the overshoot is large). If the detector is kept at a constant position, the two peaks move closer and closer together as the amplitude decreases. Eventually there will be only one peak observed. (See Figure 7, a copy of an actual record.) This coalescence is taken to indicate the time when the amplitude of the oscillation corresponds to the position of the carriage. The carriage is then displaced a few tenths of a millimeter towards smaller amplitudes, and the process is repeated. From the number of swings between coalescence for a given displacement and from the initial amplitude, the logarithmic decrement may be computed. In practice the process is repeated 30 to 40 times for each data run, and the results are averaged by a least-squares method to obtain a precise value. These calculations are programmed for MISTIC, the high-speed digital computer at Michigan State University.

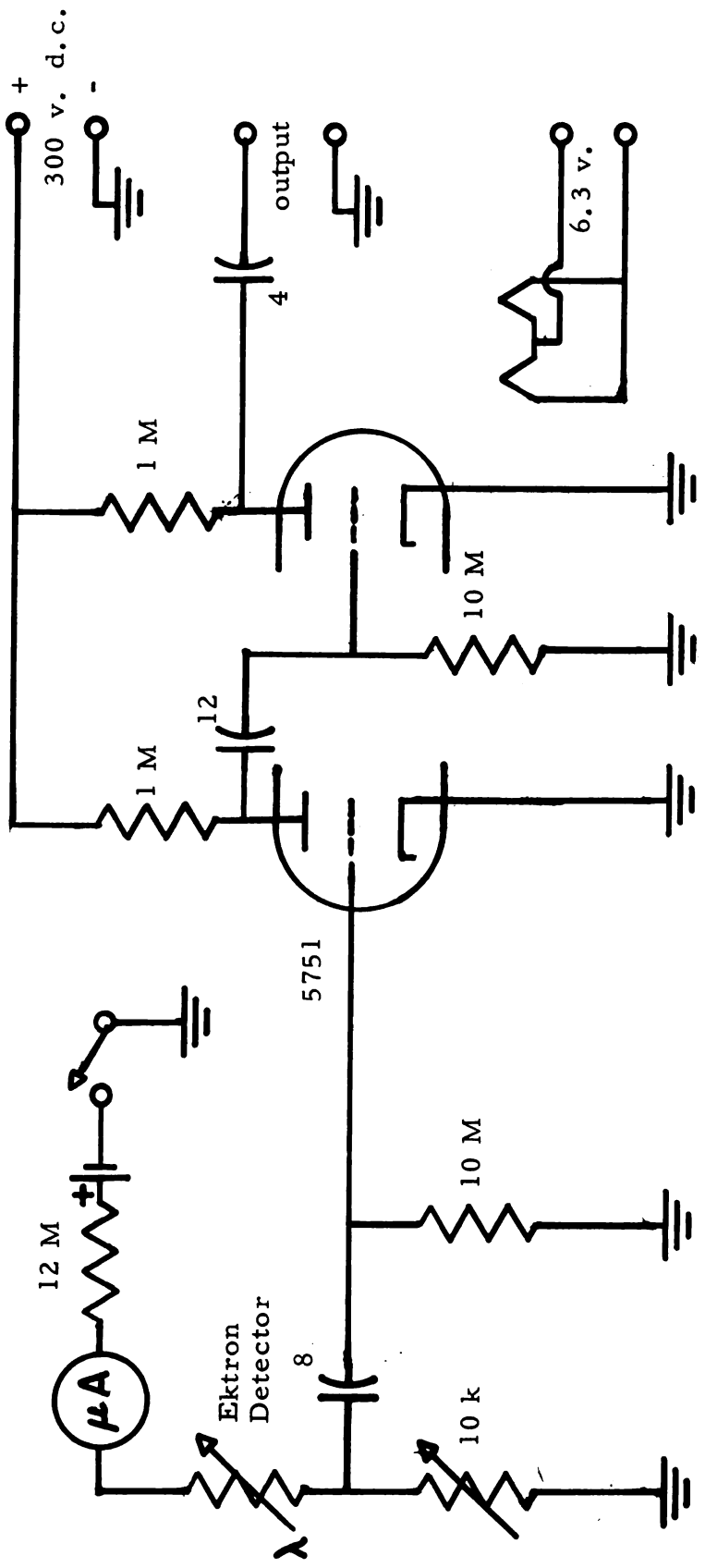

Figure 6 - Ektron Detector and Amplifier Circuit

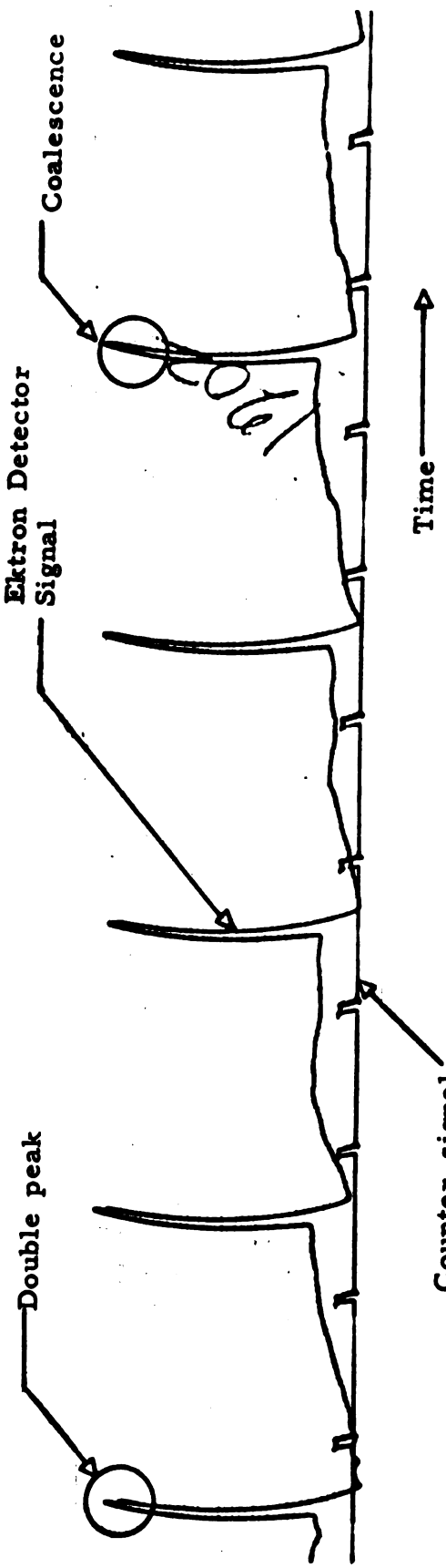

Figure 7 - Typical Record of Photocell Signals

D. Measurement of Sphere Radius

The samples of Li^6 and Li^7 for the present experiments were those used by Ban. They were maintained at all times under seal in their spheres, and it was not possible to measure the radius of the sphere without destroying the sample. Hence his values of the radius have been taken for our calculations. Ban weighed the sphere both before and after filling it with water to the top of the neck, and thence computed the volume of the cavity. The volume of the cylindrical neck, as calculated from its geometry, was subtracted from this total volume to give the volume of the spherical portion.

E. Measurement of Moment of Inertia

The geometry of the oscillating portion of the pendulum is so complicated that a precise calculation of the moment of inertia is not feasible. Therefore an experimental method has been adopted. The moment of inertia is changed by a known amount, and the effect of this change on the period is measured.

The moment of inertia of the system can be expressed as,

$$I_n = I_0 + I'_n \ , \tag{3}$$

where I_n is the total moment of inertia for a particular position of the movable masses shown in Figure 1, I_0 is the moment of inertia of the system not including the effects of the movable masses, and I'_n is the moment of inertia of the two masses as given by the parallel-axis theroem,

$$I'_n = I_{1z} + I_{2z} + M_1 d^2_{1n} + M_2 d^2_{2n}, \tag{4}$$

where I_{1z} and I_{2z} are the moments of inertia of the two masses about an axis through their center of mass and parallel to the axis of rotation of

the entire system, and M_1 and M_2 are the masses of the adjustable bodies at distances d_{1n} and d_{2n}. The distances are set such that $d_{1n} = d_{2n} = d_n$.

If the damping is small, the period of the pendulum is given by

$$T_n = 2\pi(I_n/M)^{\frac{1}{2}}.$$

Then

$$I_n = T_n^2 \, M/4\pi^2 = I_0 + I_{1z} + I_{2z} + (M_1 + M_2) \, d_n^2.$$

A similar expression holds for I_m. The two equations are solved for I_0 by eliminating M between them.

$$I_0 = -I_{1z} - I_{2z} + (M_1 + M_2) \left[\frac{(d_m^2 T_n^2 - d_n^2 T_m^2)}{T_m^2 - T_n^2} \right]$$

From equations 3 and 4 it is easy to get I_n in terms of the d's and T's:

$$I_n = (M_1 + M_2) \, T_n^2 \left[\frac{d_m^2 - d_n^2}{T_m^2 - T_n^2} \right] \qquad (5)$$

The d's are fixed by means of a special gauge block which slips over the end of the rods on which the masses slide, and moves the masses to a precise distance from the end of the rod. This rod is centered on the axis of rotation, so that use of the gauge block puts the masses at the same distance from the axis.

F. Temperature Control and Measurement

The furnace (F in Figure 1) has a 115-v, a-c, heating element wound on a ceramic frame just large enough to fit around the copper block which forms the bottom part of the vacuum enclosure and surrounds the sphere. The heating element is surrounded by a few inches of insulating material. The entire furnace is housed in a steel shell resting on the floor.

The temperature is controlled with the aid of a copper-constantan thermocouple (T in Figure 1). To keep the measured potential within the range of the controller, a portion of the voltage is backed off with a potentiometer powered by a 1-v, mercury battery. The difference between the thermocouple potential and the backing potential is applied to a Leeds and Northrup Type G Speedomax Recorder. The recorder is in turn connected to a Leeds and Northrup Series 60 Duration-Adjusting Type control unit which controls the current to the furnace by adjusting the fraction of the time the furnace is on. The Speedomax record shows that the temperature is maintained to well within $\pm$ 0.2 C-deg.

The entire temperature-measuring system is calibrated in terms of potential difference measured with a Leeds and Northrup Type K-3 Potentiometer. At each run the temperature of the furnace as measured with the K-3 Potentiometer is recorded. To find the temperature of the sphere, we need a relation between it and the furnace temperature. This calibration is obtained by attaching thermocouples to the surface of the sphere and recording their potential as a function of the furnace temperature. The corresponding temperatures are obtained by use of National Bureau of Standards Tables for Copper-Constantan Thermocouples (10).

G. Calculation

The fundamental equation (2) cannot be solved explicitly for the viscosity. The solution is obtained by iteration to the desired degree of accuracy. In the present experiment the process is continued until successive approximations differ by less than 10^{-7}, a figure well beyond the limitations of the experiment. All the calculations and corrections are included in a single program for the calculation of viscosity on MISTIC. The specific correction equations are now examined:

1. Moment of inertia: Ban has calculated that any change due to temperature is not significant.

2. Radius of the Sphere: Since the equation for calculation of viscosity is very sensitive to small changes in the sphere radius, thermal expansion of the sphere is taken into account to the first-order term:

$$R = R_{20} [1 + \alpha (t - 20)],$$

where R is the radius at 20° C, α is the coefficient of linear expansion (9.9×10^{-6}/C-deg. for type 446 stainless steel) and t is the temperature in degrees Centigrade.

3. Density: There are no values published for the density of separated isotopes of lithium as liquids. It is reasonable to assume that the atomic volume of molten lithium does not change much with isotopic mass, and hence we may deduce the values of density required from the thermal expansion and the change of volume on melting for natural lithium, as given by Bernini and Cantoni (11), Losana (12), and the values of the bulk density of the solid separated isotopes, as measured by Snyder and Montgomery (13). The densities are then given by the following formulas:

$$\rho_{Li-6} = \frac{d_{Li-6}}{1 + (174 \times 10^{-6})(t - 180.4) + (106 \times 10^{-9})(t - 180.4)^2}$$

$$\rho_{Li-7} = \frac{d_{Li-7}}{1 + (174 \times 10^{-6})(t - 180.7) + (106 \times 10^{-9})(t - 180.7)^2}$$

Here d_{Li-6} and d_{Li-7} are the densities of liquid Li^6 and Li^7 at the melting point:

$$d_{Li-6} = \frac{.460 \left[1 + (153.5 \times 10^{-6}) \times 20 + (92 \times 10^{-9})(20)^2\right]}{1.0157 \left[1 + (153.5 \times 10^{-6}) \times 180 + (92 \times 10^{-9})(180)^2\right]}$$

$$d_{Li-7} = \frac{.537 \left[1 + (153.5 \times 10^{-6}) \times 20 + (92 \times 10^{-9})(20)^2\right]}{1.0157 \left[1 + (153.5 \times 10^{-6}) \times 180 + (92 \times 10^{-9})(180)^2\right]}$$

4. Logarithmic Decrement: The residual damping occurring when the lithium is solid must be taken into account. Since this damping is small (of the order of one-twentieth of the viscous damping), the corresponding logarithmic decrement is simply subtracted from the total observed decrement.

The data presented to MISTIC are in the form of a list of 18 parameters appearing in the various equations. For each set of data there are in addition the three variables, furnace temperature (expressed in millivolts), logarithmic decrement (dimensionless), and period of the pendulum (seconds). The computer does all the intermediate calculations, and prints out the sphere temperature and the viscosity, as well as the results of intermediate calculations if desired.

CHAPTER III

SUMMARY OF PREVIOUS WORK

A. Theory

A critical review of the current theories of viscosity is given by Bondi (14). Ban reviews some of these theories, and shows from simple dimensional analysis that the expected relative change of the coefficient of viscosity η, at a constant temperature T, for a change in isotopic mass m should go as $m^{\frac{1}{2}}$. At least two of the major types of theories reviewed by Bondi (rate-process theory, and molecular theory) predict this same dependence on mass. An exponential form of the temperature dependence of viscosity, suggested many years ago by Reynolds (15) and by Guzman (16), subsequently has been used by many other workers. For a great number of liquids it seems to fit the data quite adequately (17, 18).

The present experimental work is confined to investigating the dependence of viscosity on the two parameters, isotopic mass and temperature.

B. Results

Ban's experimental results are recalled in two sections. The first section contains values of parameters connected with the experimental apparatus and relevant to the experimental work described herein. These values are reproduced here for completeness. For the methods used to obtain the detailed data, the reader is referred to appendexes A and B, and to Ban's thesis. The second section consists of the results obtained by Ban for the viscosity of Li^6 and Li^7 as a function of temperature.

1) Parameters of the Apparatus:

a) Radius of the sphere:

Li^6 sphere	1.2827 cm.
Li^7 sphere	1.2842 cm.

b) Moment of Inertia: Use of three positions of the inertia arms (d_1, d_2, d_3) with observation of the corresponding periods, T_{10}, T_{20}, T_{30}, permits three values of the moment of inertia to be calculated. The average value is taken for I, the moment of inertia. The experimental data needed are the masses, m_1 and m_2; the distances d_1, d_2, and d_3, from the axis of rotation of the inertia weights; and the periods corresponding to the different positions. The method of obtaining the masses and the distances is given in detail by Ban. The results are summarized here:

$m_1 = 189.627$ grams

$m_2 = 189.629$ grams

$m_1 + m_2 = 379.256$ grams

$d_1^2 = 5.132$ cm.^{2}

$d_2^2 = 27.716$ cm.^{2}

$d_3^2 = 18.183$ cm.^{2}

The corresponding periods are given in Appendix A.

The resulting values of I are:

Li^6:	$I = 4443.86$ gm-cm^2
Li^7:	$I = 4429.41$ gm-cm^2

c) The temperature-calibration curves are shown in Appendix B.

2) Results for Viscosity Coefficient:

Ban's results for Li^6 and Li^7 are summarized in Tables I and II. The source data are found in Appendix C. Figure 8 shows the

Table I. Viscosity of Lithium 6 (Ban)

Temperature °C	Temperature °K	Viscosity η mp	$\text{Log}_{10}\ \eta$ (mp)	$\frac{10^3}{T\ (^\circ K)}$
188.3	461.5	4.39	0.642	2.17
198.0	471.2	4.28	0.631	2.12
217.4	490.6	4.00	0.602	2.04
236.2	509.4	3.85	0.585	1.96
236.8	510.0	3.83	0.583	1.96
266.6	539.8	3.69	0.567	1.85
266.8	540.0	3.67	0.565	1.85

Table II. Viscosity of Lithium-7 (Ban)

Temperature °C	Temperature °K	Viscosity η mp	$\text{Log}_{10}\ \eta$ (mp)	$\frac{10^3}{T\ (^\circ K)}$
191.2	464.4	5.61	0.749	2.15
200.8	474.0	5.45	0.736	2.11
221.2	494.4	5.13	0.710	2.02
240.6	513.8	4.92	0.692	1.95
271.8	545.0	4.56	0.659	1.84

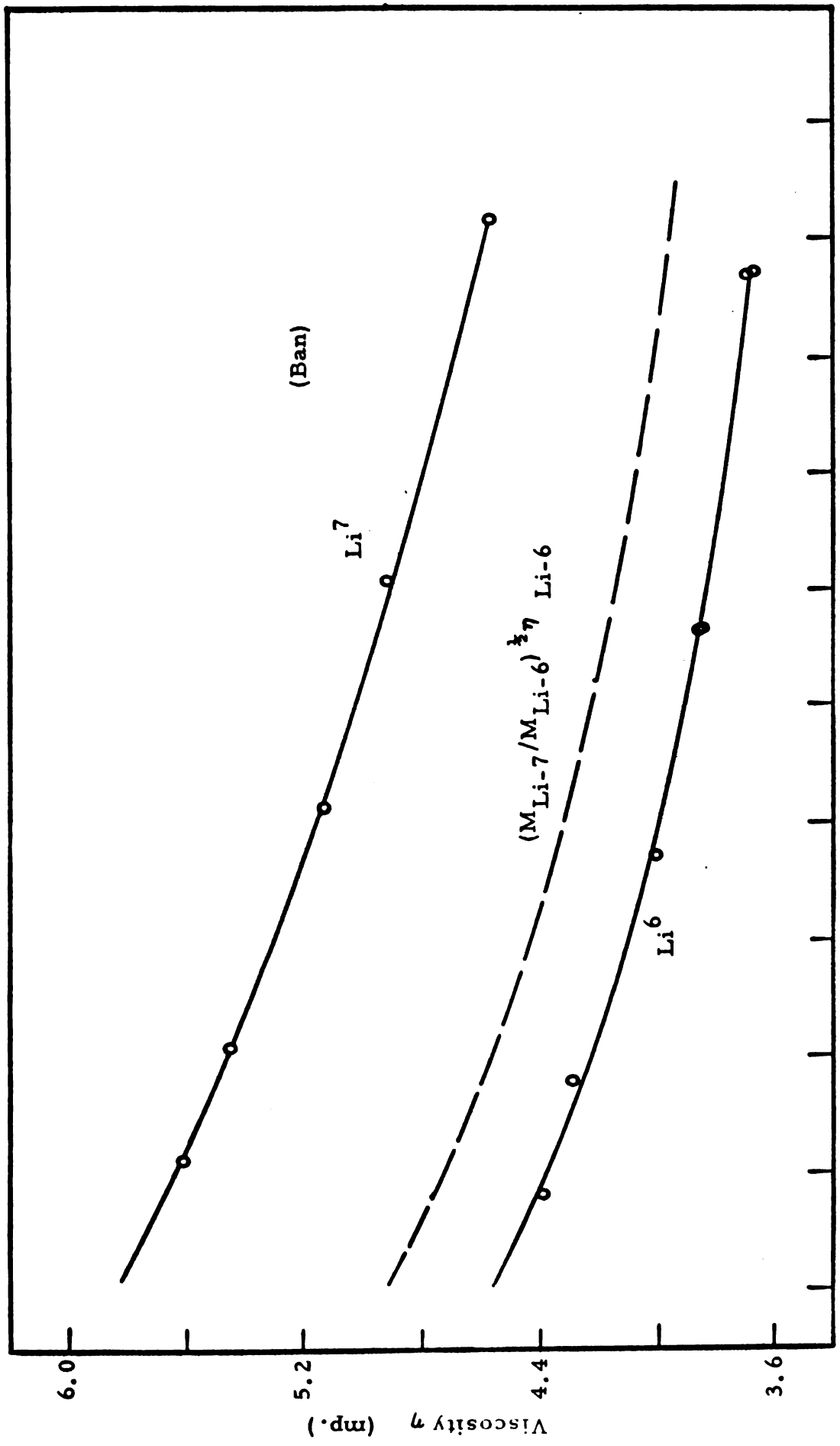

Figure 8 - Ban's values for the Viscosity η of the separated isotopes of Lithium as a function of temperature t. The dashed curve is the expected value for Li^7 from the Li^6 data obtained by multiplying the Li^6 values by the square root of the mass ratio.

experimental results for viscosity η, as a function of absolute temperature T. It shows as well the dashed curve, $\eta_{Li\text{-}6}(M_{Li\text{-}7}/M_{Li\text{-}6})^{\frac{1}{2}}$ against T. Figure 9 shows $\log_{10} \eta$ plotted against $1/T$. The resulting straight line indicates that the exponential law is adequate to express the temperature dependence. The disagreement between the curve predicted for Li^7 and the dashed curve is unresolved by Ban. It is the purpose of the present work to repeat and refine the experiment, and to re-examine the theory in an effort to reconcile this disagreement.

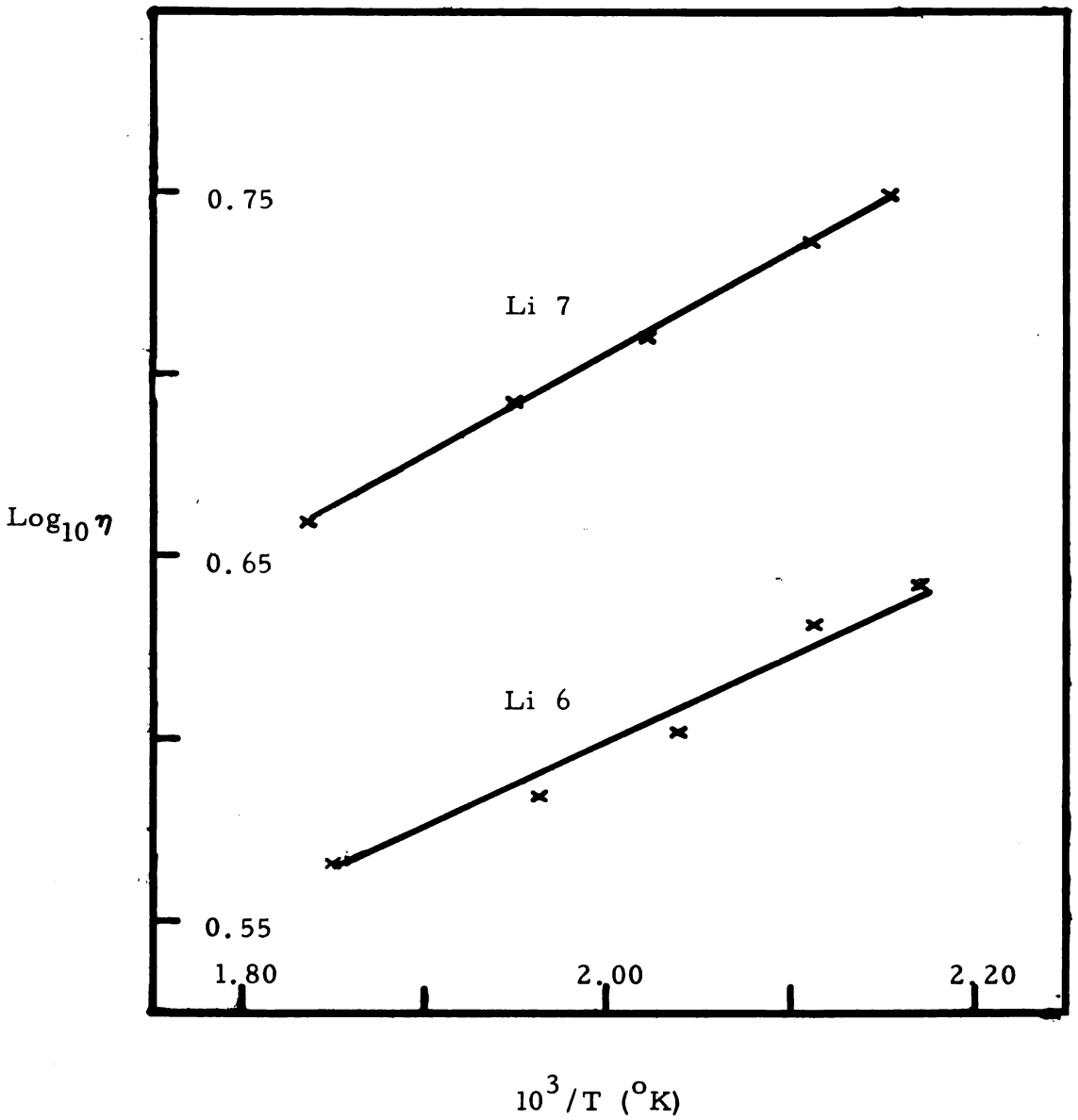

Figure 9

Log_{10} Viscosity vs Reciprocal Temperature

(Ban)

CHAPTER IV

RE-EXAMINATION OF THE EXPERIMENT

The re-examination of the experiment has two phases: 1) a careful examination of each individual measurement, and 2) a careful repetition of the entire experiment.

A. Examination of the Individual Measurements

1) Period: Time intervals were measured with an ordinary electric clock driven by a self-starting synchronous motor. On several occasions the period was measured over long intervals of time (up to 24 hours). The period during these long intervals was constant. The only possible source of error in the period measurements was the clock itself, which is synchronous with the current furnished by the Michigan State University power plant. As a check, the clock was monitored with the time signals from the local telephone company. These signals are accurate within a least one or two seconds from day to day, as determined with signals broadcast from the Naval Observatory in Washington. The monitoring showed that the clock was accurate within 1 part in 5,000, an amount less than the error in reading the clock over the much shorter lengths of time measured in the actual runs. Thus no significant error exists in the measurement of the period.

2) Logarithmic Decrement: The direct measurements involved in the calculation of this quantity are those of length of swing and of number of oscillations. The latter is obtained by counting and has no inherent error. The important requirement on the former is that the length scale be uniform and constant. Probably the best indication of the accuracy of the measurement of logarithmic decrement is its constancy from

run to run, independent of initial amplitude. Table III shows the results of experiments with Li^7, for ten runs over a period of 13 days at nominally the same temperature. Corresponding values of the viscosity coefficient have been calculated. The data have been analyzed statistically, and for what they are worth, 95% confidence limits have been established. The range of the data presented is 0.1 millipoise, and even an error as large as this extreme is not sufficient to reconcile Ban's values for Li^6 and Li^7 to the square-root dependence. Consequently, inaccuracy in this determination must be rejected as an important source of error.

3) Radius of the sphere: Ban has shown the high sensitivity of the viscosity to the radius of the sphere in the present method. Because of the high chemical reactivity of lithium, the anomalous results for Li^6 and Li^7 suggest the possibility of some sort of reaction between the lithium and the sphere, with consequent changes in the dimensions and the shape of the sphere, and in the density of the liquid metal. Moreover, a great increase in the viscosity of liquid metals upon the addition of small amounts of metallic impurities has been reported (19). Finally, the difference between Ban's values for lithium-7 and the present values suggest that some change may be taking place over a long period of time.

The search for existence of corrosion was examined by two methods: 1) the lithium was analyzed for the constituents of the stainless steel, and 2) the radius of the sphere was remeasured. Since the analysis is destructive, only one sample, Li^7, was tested.

The stainless-steel sphere containing the lithium was heated on a small electric hot plate under an argon atmosphere.* The molten lithium was transferred to a weighed nickle crucible by displacing it with argon forced into the sphere through a stainless-steel tube inserted into

---

*A controlled-atmosphere enclosure was kindly made available by Dr. H. A. Eick of the Department of Chemistry at Michigan State University.

Table III. Decrement at Constant Temperature Lithium-7 (Randall)

Date	Temperature T Furnace (mv)	Temperature T Sphere (°C)	Logarithmic Decrement δ	Viscosity η (mp)
6/20/61	9.9715	187.1	578.484	5.88
6/23/61	9.9794	187.2	577.040	5.84
6/21/61	9.9805	187.2	580.143	5.94
6/19/61	9.9867	187.3	577.179	5.83
6/22/61	9.9869	187.3	576.269	5.80
6/15/61	9.9929	187.5	577.338	5.83
6/25/61	10.0021	187.6	577.354	5.84
6/26/61	10.0029	187.6	576.892	5.83
6/13/61	10.0038	187.7	577.338	5.84
6/16/61	10.0087	187.7	579.200	5.91

Statistical Analysis of Logarithmic Decrement

Mean 577.7×10^{-6}

Standard Deviation 1.18×10^{-6}

95%-Confidence Interval $(577.7 \pm 2.32) \times 10^{-6}$

Statistical Analysis of Viscosity

Mean 5.85 mp

Standard Deviation 0.014 mp

95%-Confidence Interval (5.85 ± 0.014) mp

the sphere through the neck. When the lithium had cooled, the crucible was reweighed in the controlled-atmosphere enclosure. The crucible containing the lithium was placed in a desiccator which was then removed from the argon atmosphere. There was some question concerning the weighings made in the dry box, because the balance could not be closed and the pans may have been disturbed by atmospheric currents set up by the hot plate. In view of this uncertainty, the crucible with the lithium was later quickly transferred from the desiccator to a single-pan balance and reweighed. The results differed from those made in the controlled atmosphere by only slightly more than 0.1 percent.

The crucible and the lithium were then placed in a 600 ml. beaker. Water was added slowly until all the lithium had reacted to form the hydroxide. The resulting liquid was filtered through a sintered-glass funnel and made up to standard volume. The funnel was then washed with hot nitric and hydrochloric acids, and the resulting solution was analyzed to detect any materials that might have been not in actual solution in the lithium but rather in the form of inclusions. The small amount of lithium remaining in the sphere was also reacted with water. After the resulting lithium hydroxide was removed, the sphere was washed with acid (dilute HCl and HNO_3). The four solutions thus obtained were analyzed separately by colorimetric methods for the major constituents of the type-446 stainless steel, namely, iron, chromium, and nickel. The amounts in the individual analyses are added to get the total quantity of each element present.

Chromium was determined by oxidizing the chromium to valence six and forming a soluble red-violet product with di-phenylcarbazide in acid solution.* The iron was determined by the formation of a red complex

---

*The analytical procedures were selected and carefully carried out by Mr. Richard Haire of the Department of Chemistry at Michigan State University.

between 0-phenanthroline and the ferrous ion, in a controlled-pH solution. Nickel was determined by forming nickel (II) dimethylglyoxime and extracting it into chloroform (20).

The results of the analysis are presented in Table IV. The amounts listed represent upper limits only, since the contamination was so slight that the color changes were difficult to detect. The first section of the table includes the results from all four solutions. Since there was possibly attack of the stainless steel in the acid washing, there is some question whether the analysis of this solution should be included in the total metals found. Therefore the data excluding the contributions from the final washings of the sphere are presented in the second part of the table.

The original semi-quantitative spectrographic analysis supplied by Oak Ridge is not available. Analyses of the Li^6 sample and of an earlier Li^7 sample, however, are available. They indicate the possibility of an even greater amount of contamination than that found in the present analysis. These negative results lead us to believe there has been no significant contamination of the lithium by the stainless steel.

As an additional check the radius of the sphere was remeasured, by a slightly different technique from that of Ban. The sphere is filled with fluid in small precisely measured amounts, and the corresponding change in the height of the fluid, h, is noted. If $3V/\pi h^2$, where V is the cummulative volume of the fluid in a vessel, is plotted versus the height, h, the result for any ellipsoid of revolution about a vertical axis is a straight line. If the ellipsoid is a sphere, the slope of the line is minus one. This procedure then tells something about the shape of the cavity as well as its dimensions, which can be found from the intercepts of the straight line. For a true sphere either intercept is equal to three times the radius.

Table IV. Chemical Analysis of Lithium-7 After Measurements
Sample size 4.80 grams

Material	Maximum Amount Present grams	Percent
Including Acid wash of sphere		
Iron	1×10^{-3}	0.02
Nickel	6×10^{-4}	0.01+
Chromium	3.4×10^{-4}	0.007
Excluding Acid wash of sphere		
Iron	6×10^{-4}	0.01
Nickel	5×10^{-4}	0.01
Chromium	3×10^{-4}	0.006

For measuring, the sphere was attached to a milling-machine bed to obtain calibrated vertical motion as well as convenient motion in a horizontal plane. A vertical rod was passed into the sphere, clearing the neck and serving as an electrode to contact the surface of the liquid. The height of the liquid was determined by raising the sphere until the electrode touched the surface of the liquid, and triggered a thyratron actuating a relay. The liquid was added from a 5-ml. precision bore burette.

The results of a typical measurement for volume, V, as a function of height, h, are shown in Figure 10. Figure 11 gives the same data in different form with $3V/\pi h^2$ plotted against h. The filling liquid was water, with 0.1% wetting agent (an aerosol) added. The best-fitting line (shown dashed) is slightly less steep than a line of slope minus-one drawn through the points (shown dot-dash). Another line (shown solid) is obtained upon assuming the container to be a true sphere of the radius measured by Ban (1.28 cm). Examination suggests a radius slightly larger (1.30 cm). Repetition of the measurements, however, with mercury instead of water (Figure 12) gives a radius slightly smaller (1.25 cm). It seems more reasonable then to explain the divergence between measurements through interfacial tension of the liquid to the walls, rather than by a long-term increase in the size of the chamber. Interfacial tension gives rise to a positive contact angle in the case of water, and a negative contact angle in the case of mercury. The bracketing of Ban's value by our values leads us to believe that there has been no significant change in the radius of the sphere during the experiments.

In summary, there seems to be no reason to suspect occurrence either of long-term change in the radius of the sphere, or of contamination of its contents, for the following reasons:

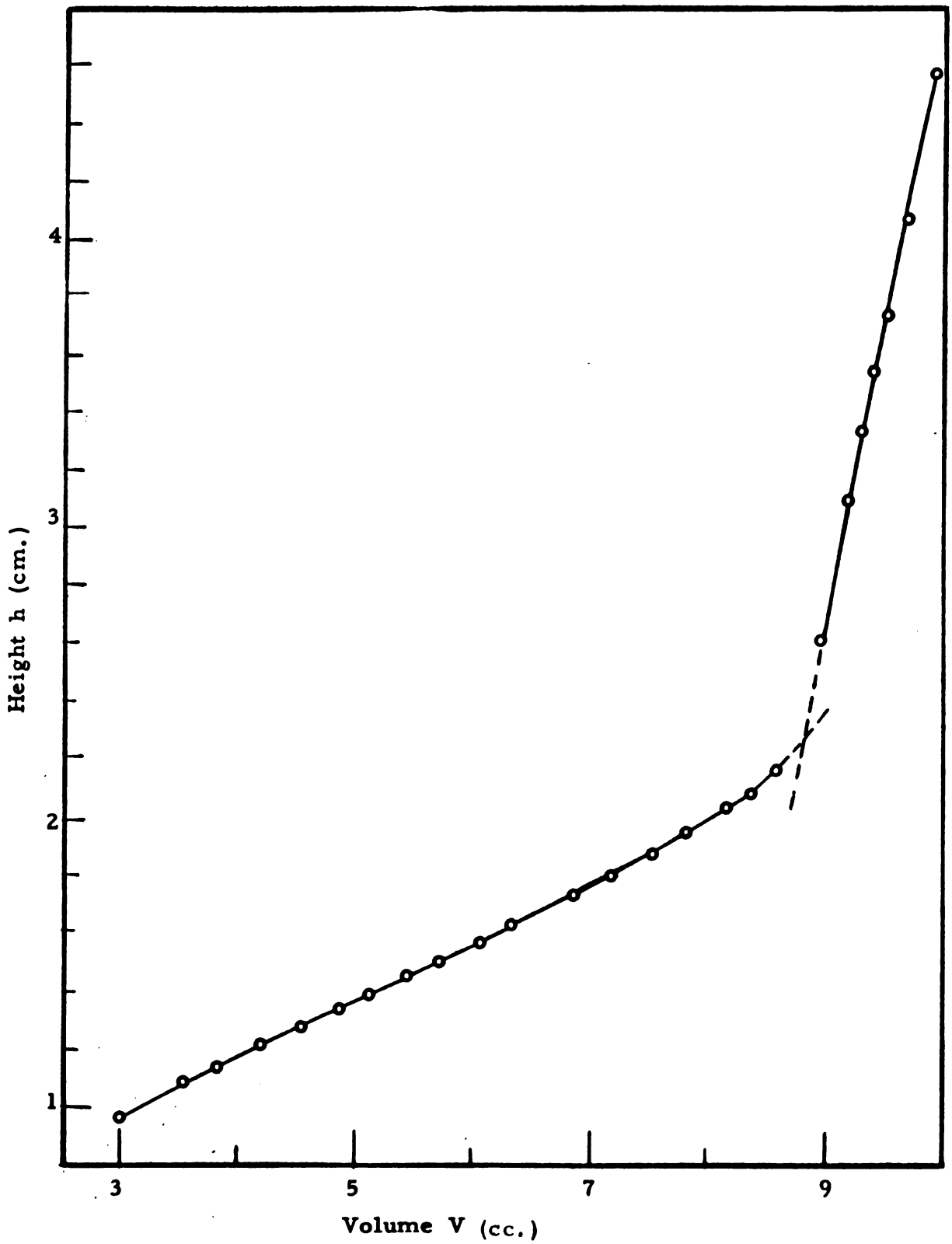

Figure 10 - Height h of fluid (water) as a function of the cumulative volume V of fluid added for the Li^7 sample container.

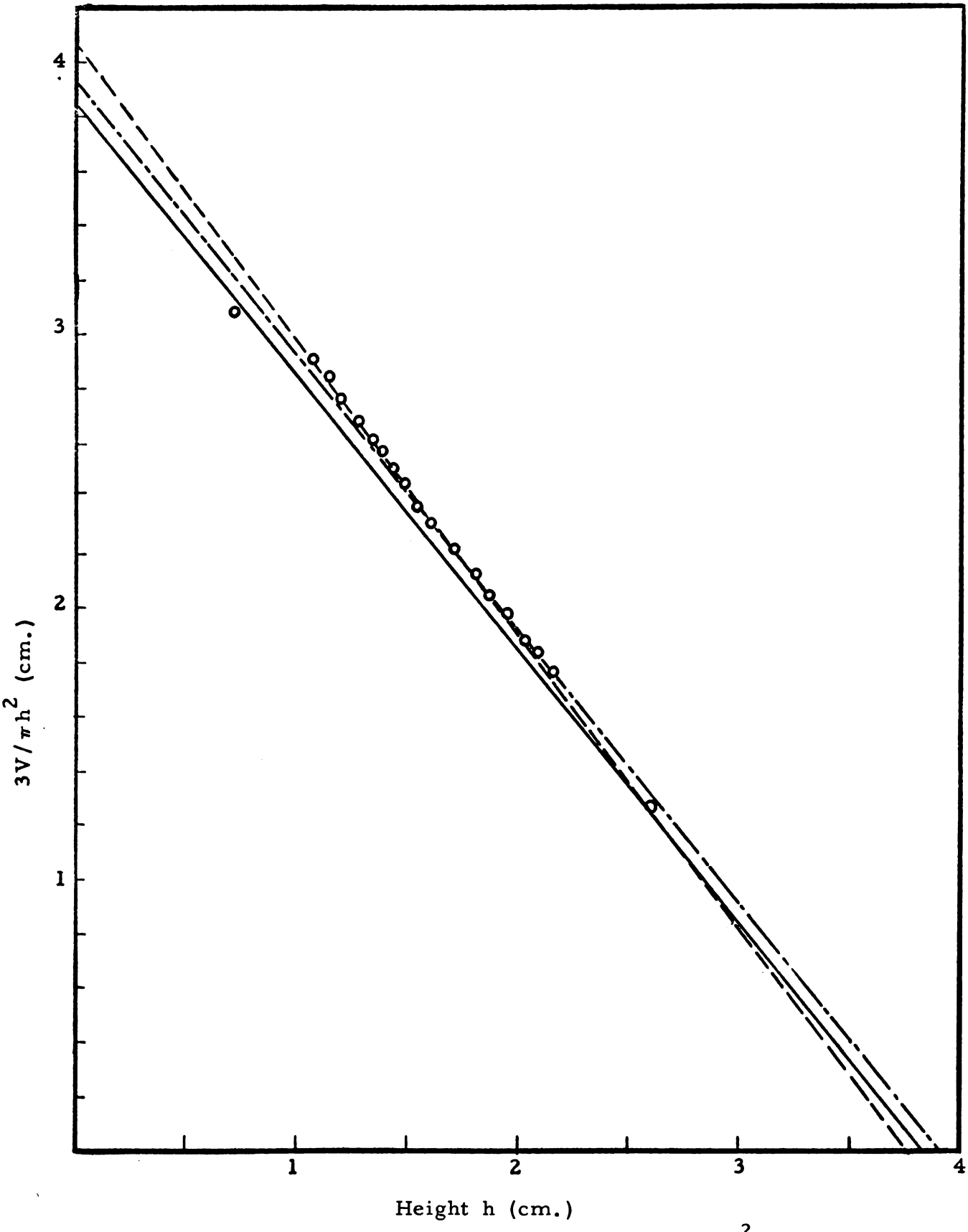

Figure 11 - The data of figure 10, plotted with $3V/\pi h^2$ against height h of fluid (water). The dashed line is a straight line through the experimental points. The dot-dash line is a line of slope minus one through the points. The solid line is the curve expected for a sperical container of the volume measured by Ban.

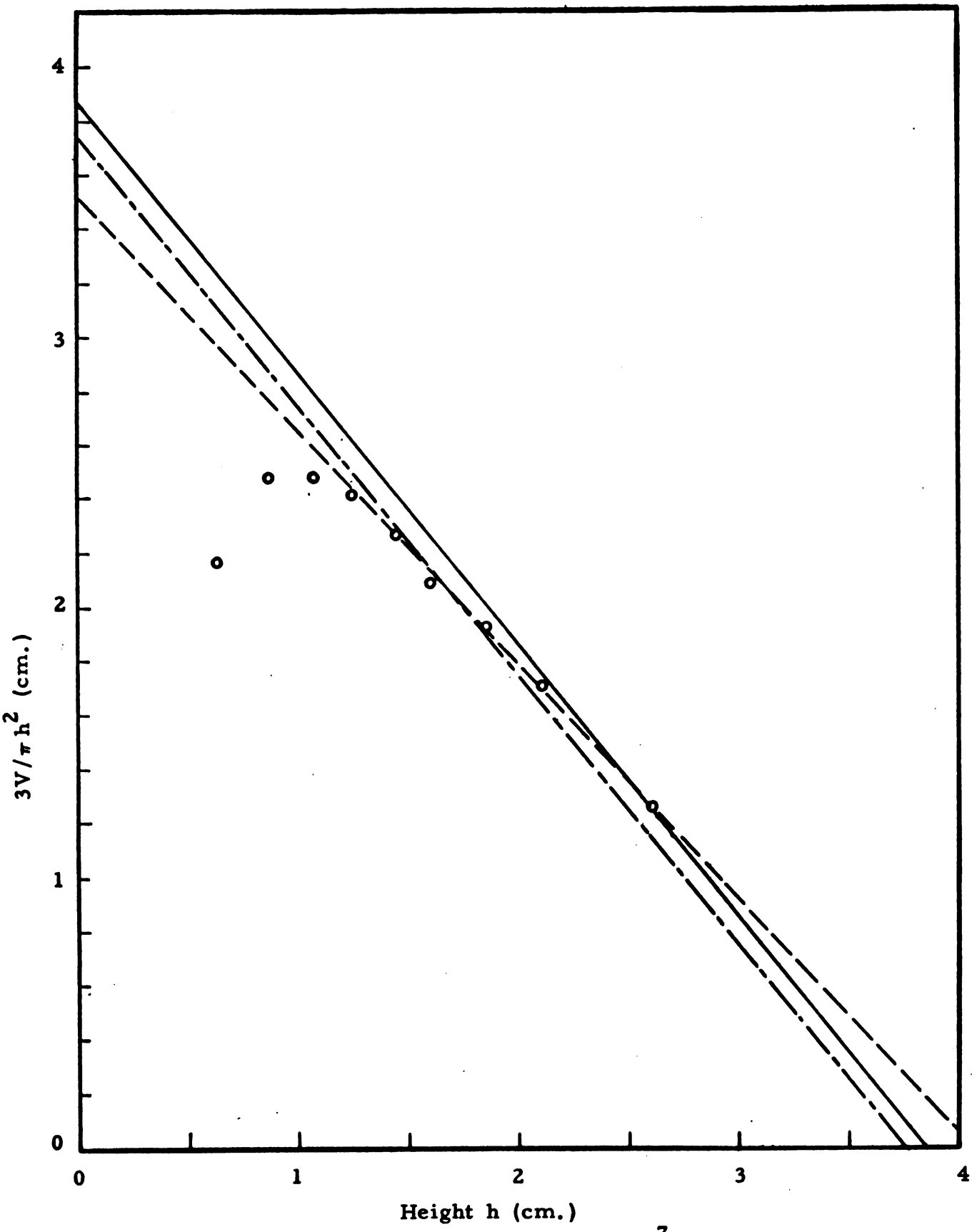

Figure 12 - The results of filling the Li^7 sample container with mercury plotted with $3V/\pi h^2$ against height h. The dashed line is a straight line through the experimental points. The dot-dash line is a line of slope minus one through the points. The solid line is the curve expected for a spherical container of the volume measured by Ban.

a) Measurement of volume versus height gives no indication of an increase in the radius.

b) Analysis of the lithium shows that the constituents of the stainless steel are not present in the lithium to any greater extent than they were in the original sample.

c) The Li^6 sample, which has been in its container for several months longer than the Li^7 sample, shows no significant long-period change in viscosity.

4) Moment of inertia: The calculation of the viscosity coefficient is not critically dependent on I, the moment of inertia of the oscillating system. The moment of inertia for the Li^6 sphere was redetermined, however, as a check on the reproducibility of this measurement. The method of calculation is the same as that adopted by Ban. The results are summarized in Table 5.

When the average value for I from Table V is compared with Ban's value, there is less than 0.3% difference. This difference would have only a very slight effect on the viscosity coefficient.

5) Density: The values of this parameter were deduced from the work of others (11, 12, 13), and were not checked experimentally. The atomic volumes for Li^6 and Li^7 differ by only a few hundred parts per million at room temperature, and surely by considerably less at temperatures above the melting point. The atomic masses are very closely in the ratio of mass numbers. The density for natural lithium is well established, and even significant errors in its value would not affect the ratio of the densities of the separated isotopes.

6) Temperature: The temperature is measured by indirect means, and there is a possibility of appreciable error in this measurement. But it is extremely unlikely that the error could amount to the approximately 60 C-deg. necessary to reconcile the viscosity measurements with the simple theory.

Table V. Determination of Moment of Inertia Lithium-6 (Randall)

Period	(Distance)^2
T_{10} = 8.8098 sec.	d_1^2 = 5.13204 cm^2
T_{20} = 12.8078 sec.	d_2^2 = 27.71601 cm^2
T_{30} = 15.0720 sec.	d_3^2 = 18.18255 cm^2

Results

Distance Used	Moment of Inertia
With d_1 and d_2	I = 4,444.58 gm-cm^2
With d_1 and d_3	I = 4,444.84 gm-cm^2
With d_2 and d_3	I = 4,446.17 gm-cm^2
Average value	I = 4,445.20 gm-cm^2

Fortunately the calibration point at melting can be ascertained directly, since the melting points of the separated isotopes are known (21). The damping should increase sharply when the lithium melts. The abrupt rise is shown for Li^6 in Figure 13 and for Li^7 in Figure 14. In each case the abscissas are taken as furnace temperature (in millivolts) and sphere temperature (in degrees Centigrade) as given by the calibration relation. The melting point is shown by a vertical line.

During the calibration experiments the temperature of the sphere was continuously monitored. Equilibrium was attained about 16 hours after the furnace was first turned on. For a 1-mv equivalent change in temperature, about 12 hours were required for the sphere to come to equilibrium.

Summary: A careful examination of the individual measurements reveals no source of error of the magnitude necessary to reconcile the experimental results with the predictions of simple theory.

B. Repetition of the Entire Experiment

The results for Li^6 and Li^7 are summarized in Tables VI and VII, respectively. The data from which the values were derived are tabulated in Appendix D. Here each entry for the logarithmic decrement represents one run in which the logarithmic decrement was obtained at about every half millimeter over a decrease in amplitude of about 20 millimeters at an initial swing of 20 cm. Thus, thirty to forty points were available from which the average logarithmic decrement could be obtained. The runs were usually spaced about a day apart to make sure that sufficient time had elapsed for temperature equilibrium to be achieved. To verify attainment of equilibrium, two consecutive runs were made at each temperature. The consistency of such data attests to the constancy of the temperature.

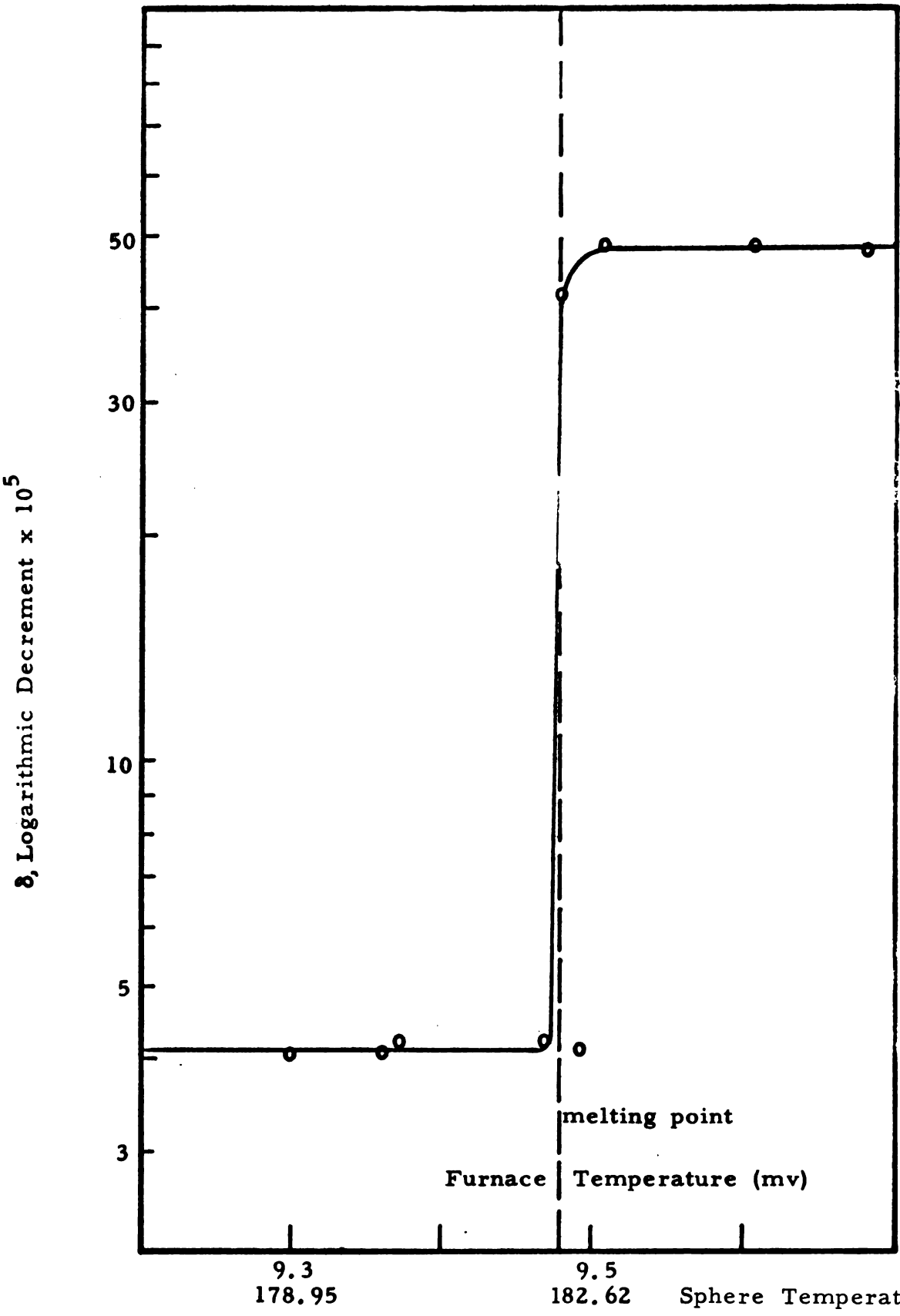

Figure 13 - Logarithmic decrement δ as a function of temperature for Li^6. The melting is evidenced as an abrupt increase in the decrement when the melting temperature (180.4°C) is reached. The upper abscissa scale is the furnace temperature in millivolts; the lower scale is the sphere temperature as given by the calibration relation.

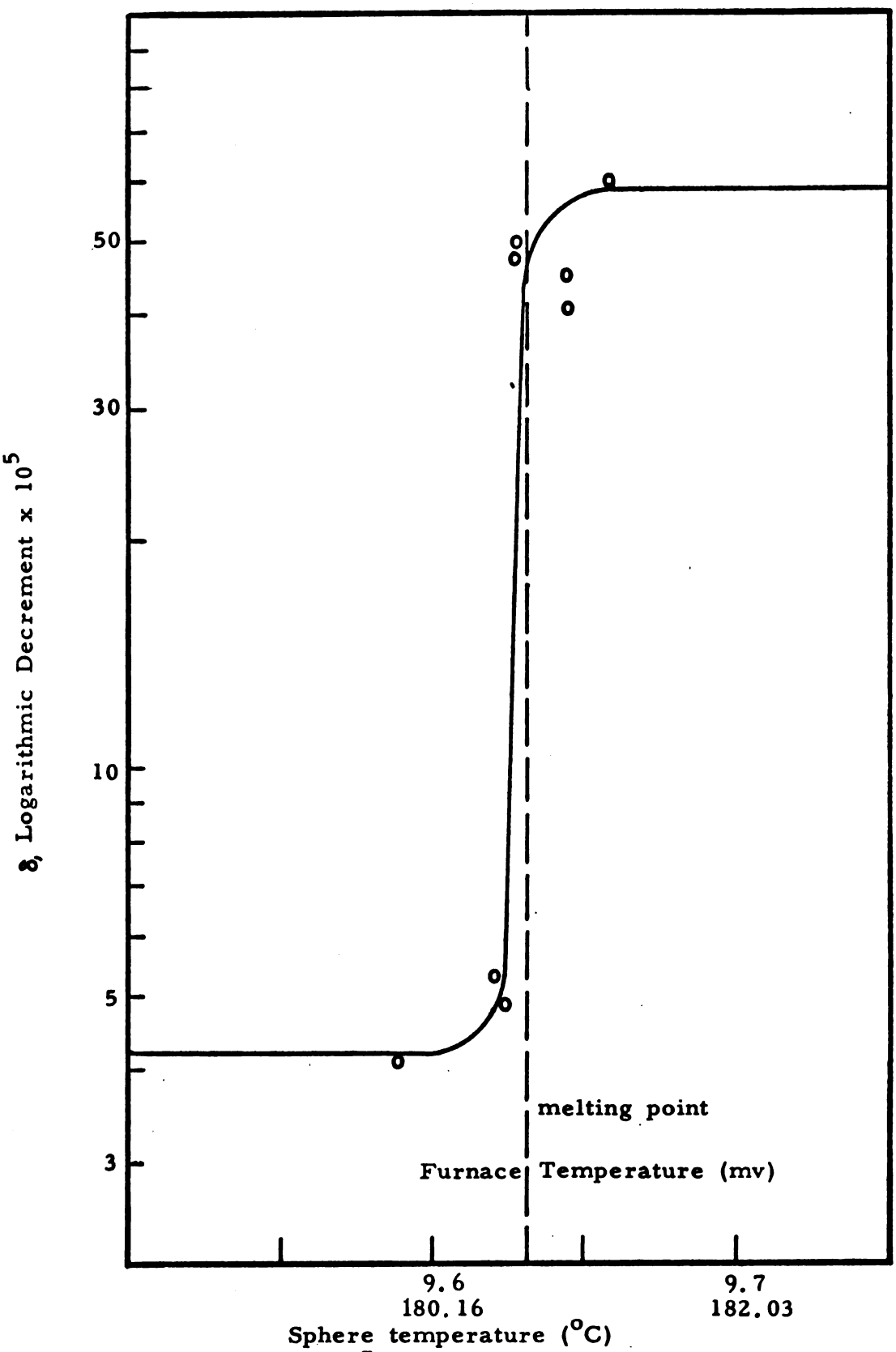

Figure 14 - The melting of Li^7 is observed as an abrupt increase in the logarithmic decrement when the melting temperature (180.7°C) is reached. The upper abscissa scale is the furnace temperature in millivolts; the lower scale is the sphere temperature as given by the calibration relation.

Table VI. Viscosity of Lithium-6 (Randall)

Temperature $T_{°C}$	Temperature $T_{°K}$	Viscosity η mp	$\text{Log}_{10}\ \eta$	$\frac{10^3}{T(°K)}$
182.4	455.6	4.20	0.623	2.195
188.2	461.4	4.14	0.617	2.167
198.2	471.4	4.14	0.617	2.121
203.7	476.9	4.04	0.606	2.097
221.3	494.5	3.93	0.594	2.022
243.3	516.5	3.77	0.576	1.936
265.4	538.2	3.63	0.560	1.858
267.1	540.3	3.60	0.556	1.851
287.4	560.6	3.48	0.542	1.784

Table VII. Viscosity of Lithium-7 (Randall)

Temperature T		Viscosity η	$\text{Log}_{10}\ \eta$	$\frac{10^3}{T(^oK)}$
^oC	^oK	mp		
184.8	458.0	5.88	0.769	2.183
185.6	458.8	5.97	0.776	2.180
186.7	459.9	5.86	0.768	2.174
187.5	460.7	5.89	0.770	2.171
199.6	472.8	5.71	0.757	2.115
215.3	488.5	5.41	0.733	2.047
238.8	512.0	5.12	0.709	1.953
240.2	513.4	5.15	0.712	1.948
264.2	537.4	4.84	0.685	1.861
265.7	538.9	4.79	0.680	1.856
286.3	559.5	4.61	0.664	1.787

The results presented in Tables VI and VII along with Ban's results are plotted in Figures 15 and 16. The agreement is good, especially in the case of Li^6. The average between Ban's work and the present work is also shown (dot-dash). The fit of the present data to the exponential law can be seen in Figure 17, where the logarithm of the viscosity is plotted against reciprocal temperatures for both isotopes.

Figure 18 shows the average curves for lithium-6 and lithium-7 along with the curve for the former multiplied by the square root of the mass ratio. The results are not significantly different from those given by Ban (Figure 8).

Our examination of the individual measurements and the corroboration of Ban's findings, upon our repetition of the experiment lead us to believe that the experiment has been conducted with proper care.

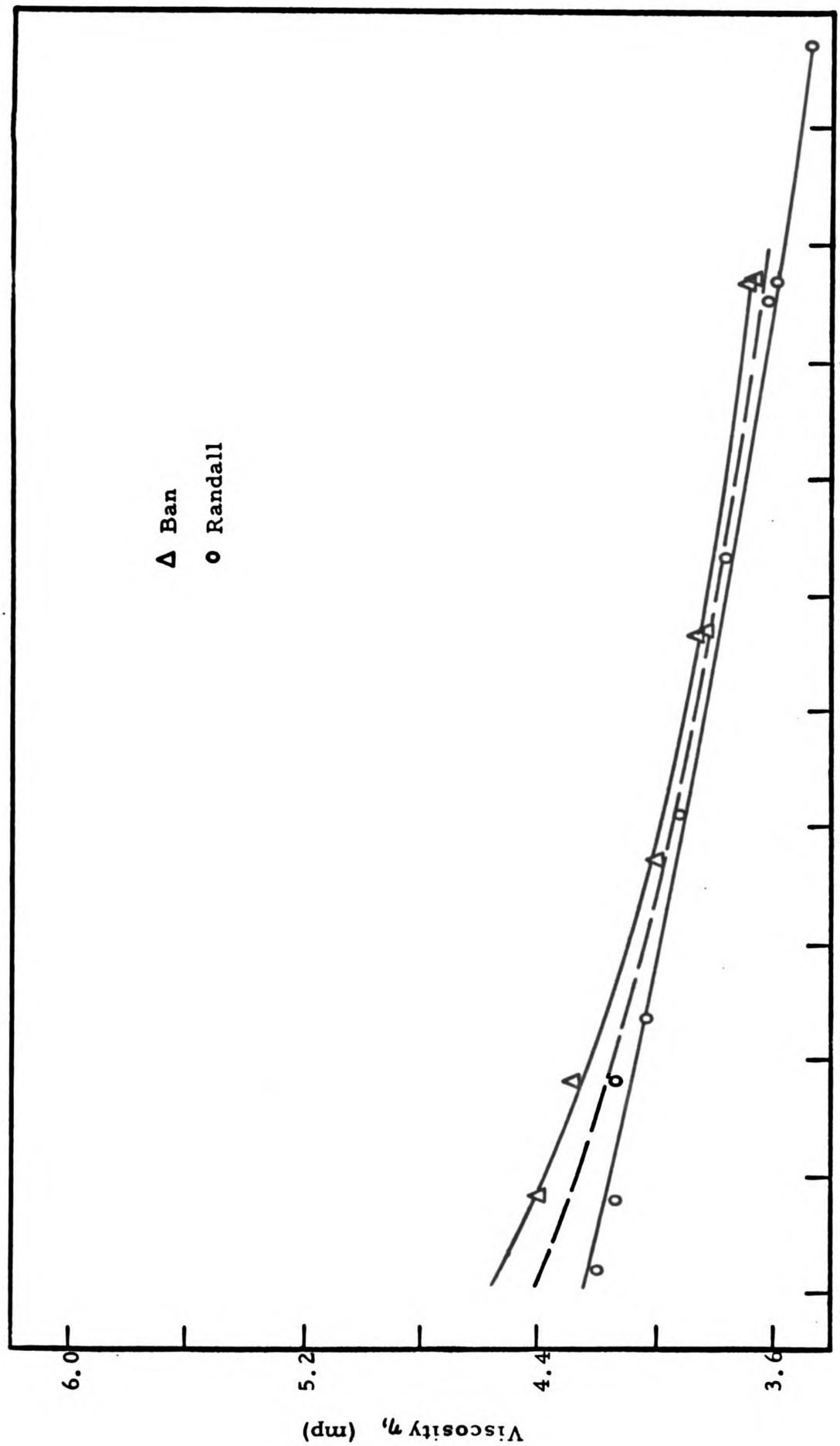

Figure 15 - The viscosity η, of Li^6 as a function of temperature t, as found in Ban's work and in the present work. The dashed curve is an average between the two curves.

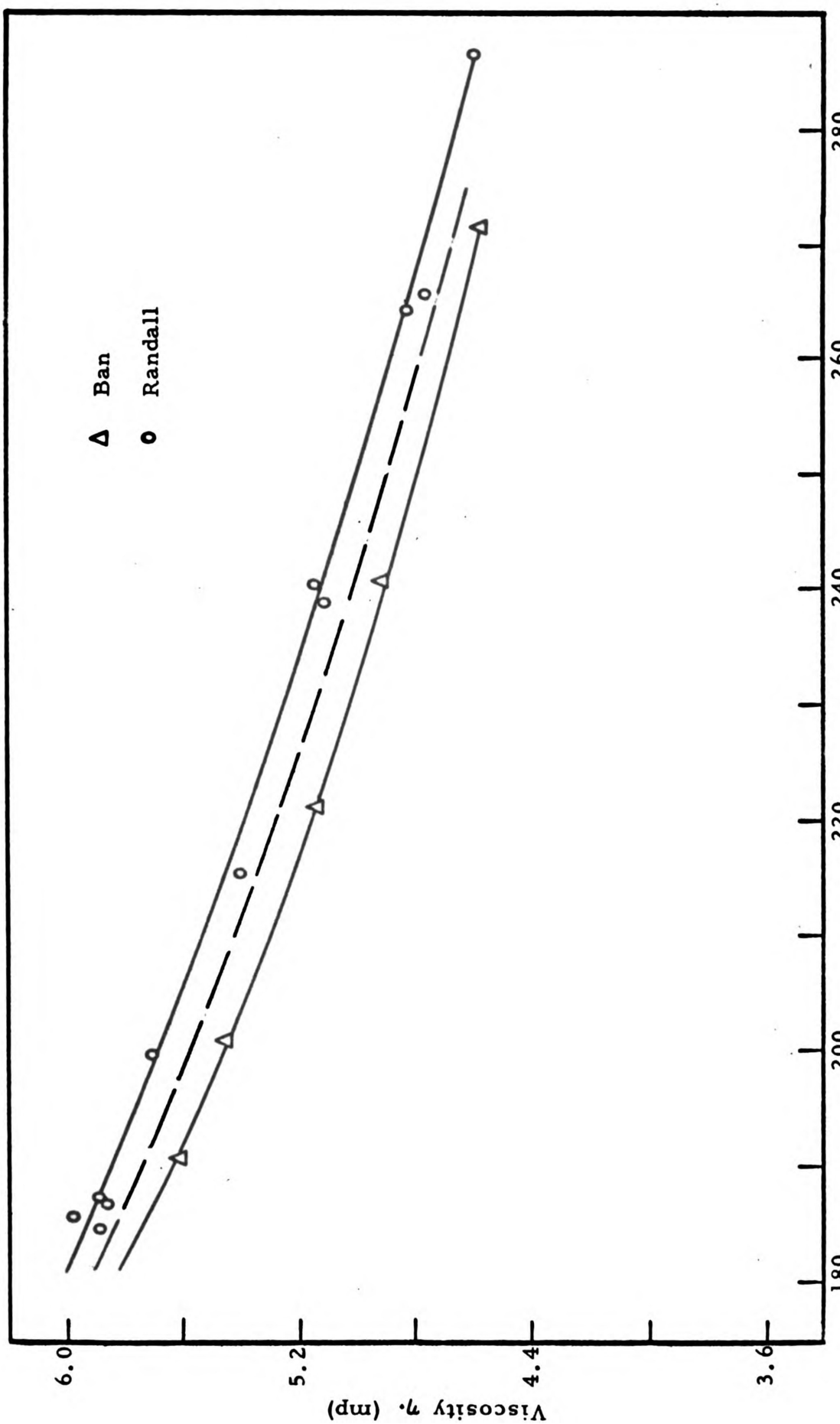

Figure 16 - The viscosity η, of Li^7 as a function of the temperature t, as found in Ban's work and in the present work. The dashed curve is an average of the two curves.

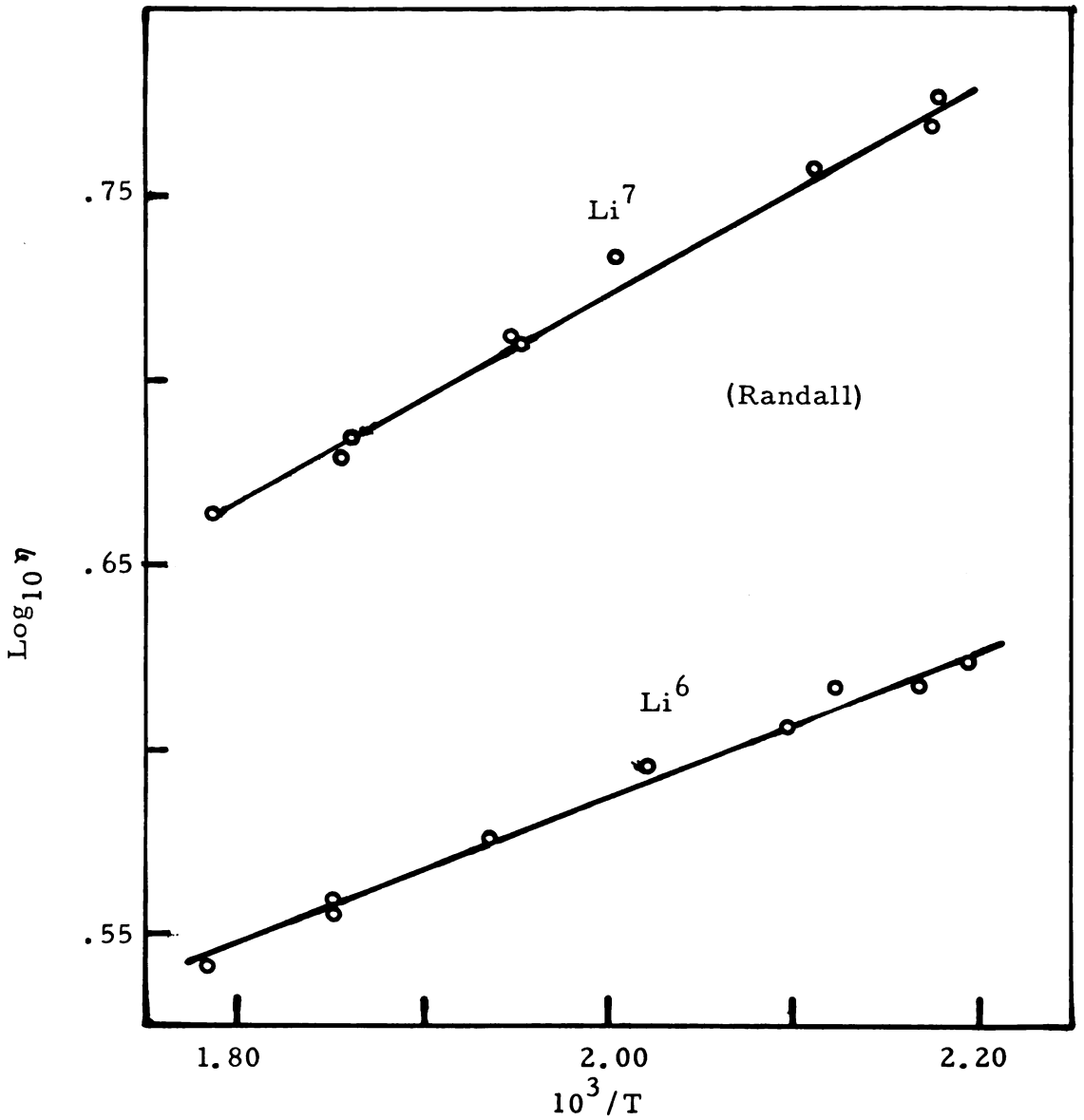

Figure 17 - Results of the present work in the form of the logarithim of the viscosity as a function of the reciprocal absolute temperature.

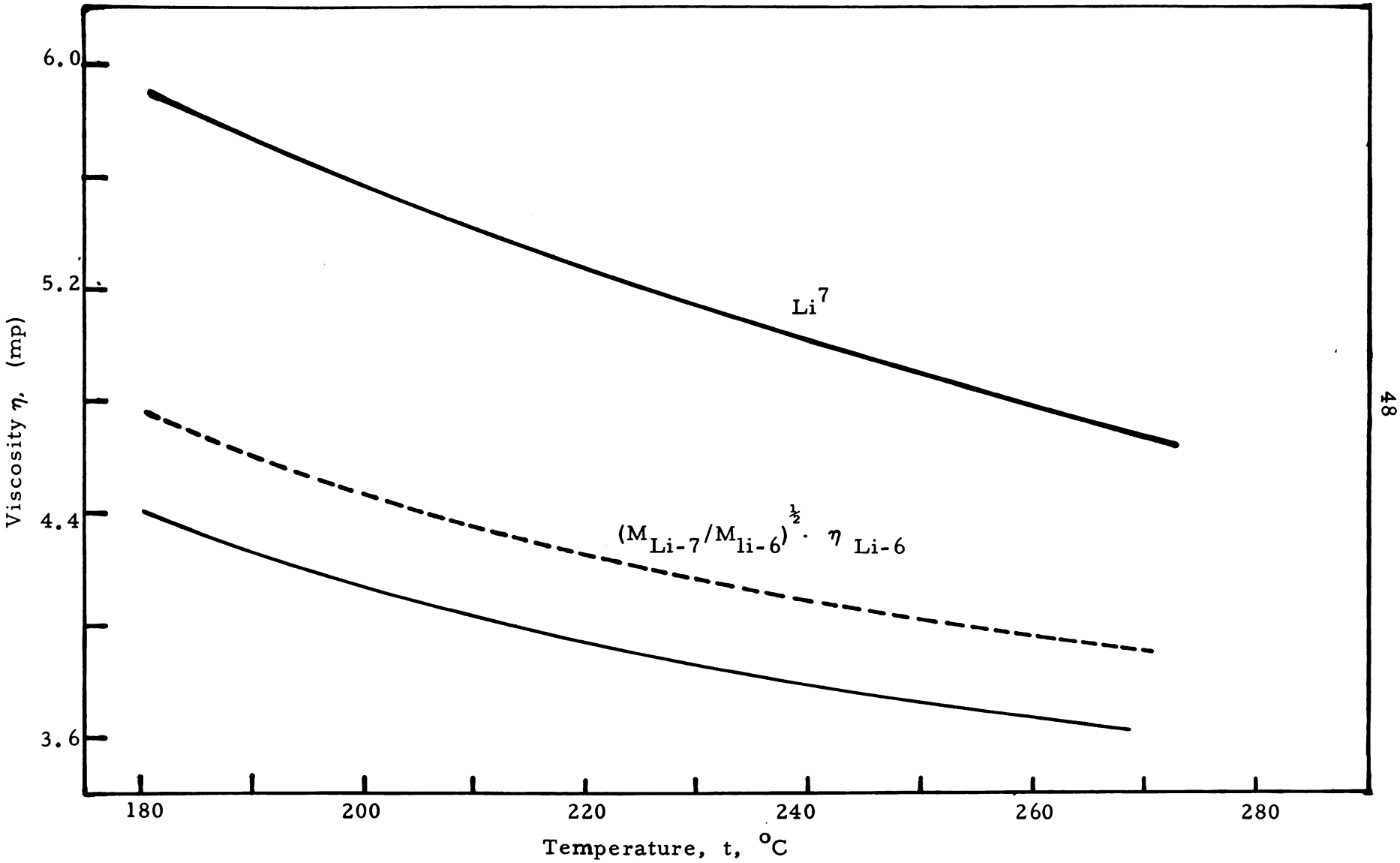

Figure 18 - The average curves of figures 15 and 16 as a function of temperature. The dashed curve is the expected value for Li^7 from the Li^6 data obtained by multiplying the Li^6 values by the square root of the mass ratio.

CHAPTER V

CONCLUSION

A careful re-examination of the experimental method has failed to reveal any serious sources of error. Repetition of the experiment gives essentially the same results as those found by Ban, leaving us with values of the viscosity that do not agree with a simple dependence on the square root of the mass. There are two explanations: First, the principle of the experimental method is not correct, but with the present form of the apparatus such an explanation does not seem likely. Andrade and Dobbs (2) with this type of apparatus have obtained values for the viscosity of natural lithium (92.6% Li^7, 6.4% Li^6) which are not in severe disagreement with the present results obtained with Li^7. These workers have measured the viscosities of a number of other materials and obtained results which agree with published values (22). Ban has measured the viscosity of water with the present apparatus, obtaining values only a few percent lower than the accepted values (Appendix E).

The second explanation is that the theory is not sufficiently developed to predict the results of the substitution in isotopic mass. The liquid state is less susceptible to theoretical attack than either the crystalline or gaseous state. In crystals the interactions are persistent, but the order is high. In gases the disorder is high, but the interactions are infrequent. In liquids there is the unhappy combination of high disorder with constant interaction between any particle and several neighbors.

Ban has reviewed some of the theories of the liquid state. None of them can be applied directly to predict the effect of isotopic mass on

viscosity at moderate temperatures. Consequently we resort to general arguments such as those of dimensional analysis. The results of a careful analysis of this type on the problem at hand do not seem to have been published.

Consider a fixed number of spherically-symmetric particles each of mass, m, and in a container of volume v, at a temperature T, and under an external pressure p. Let the interaction of the particles be described by a potential function ϕ (r) representing perhaps a weak attraction at large distances and a strong repulsion at short distances. (See Figure 19.) We characterize the potential by two parameters, the first a spatial coordinate representing a range of some kind, the second an energetic coordinate representing a depth of some kind. For convenience, we take as the former s, the distance of the potential minimum from the center of the particle, and we take as the latter b, the second derivitive of the potential curve evaluated at the minimum, recognizing that for curves of a fixed form the depth of the well and the second derivative of the function at the bottom are proportional. The parameter b has the interpretation, of course, of the spring constant for an oscillator in the harmonic approximation.

We now apply the methods of dimensional analysis to this model (23), which in the present form could apply to any state of matter. We shall consider as the parameters likely to appear in the equations of motion for the system the set m, b, and s, characterizing the individual particles; the set p, v, and T, characterizing the conditions of the system; and $\hbar$ (Planck's constant) which will enter when any quantum effects are present. The fundamental variables could have been taken as mass, length, time, and temperature; however, such a procedure merely introduces another constant, k (Boltzman's constant), and complicates the algebra without yielding additional information. We believe it is better just to take kT together in the form of a thermal energy.

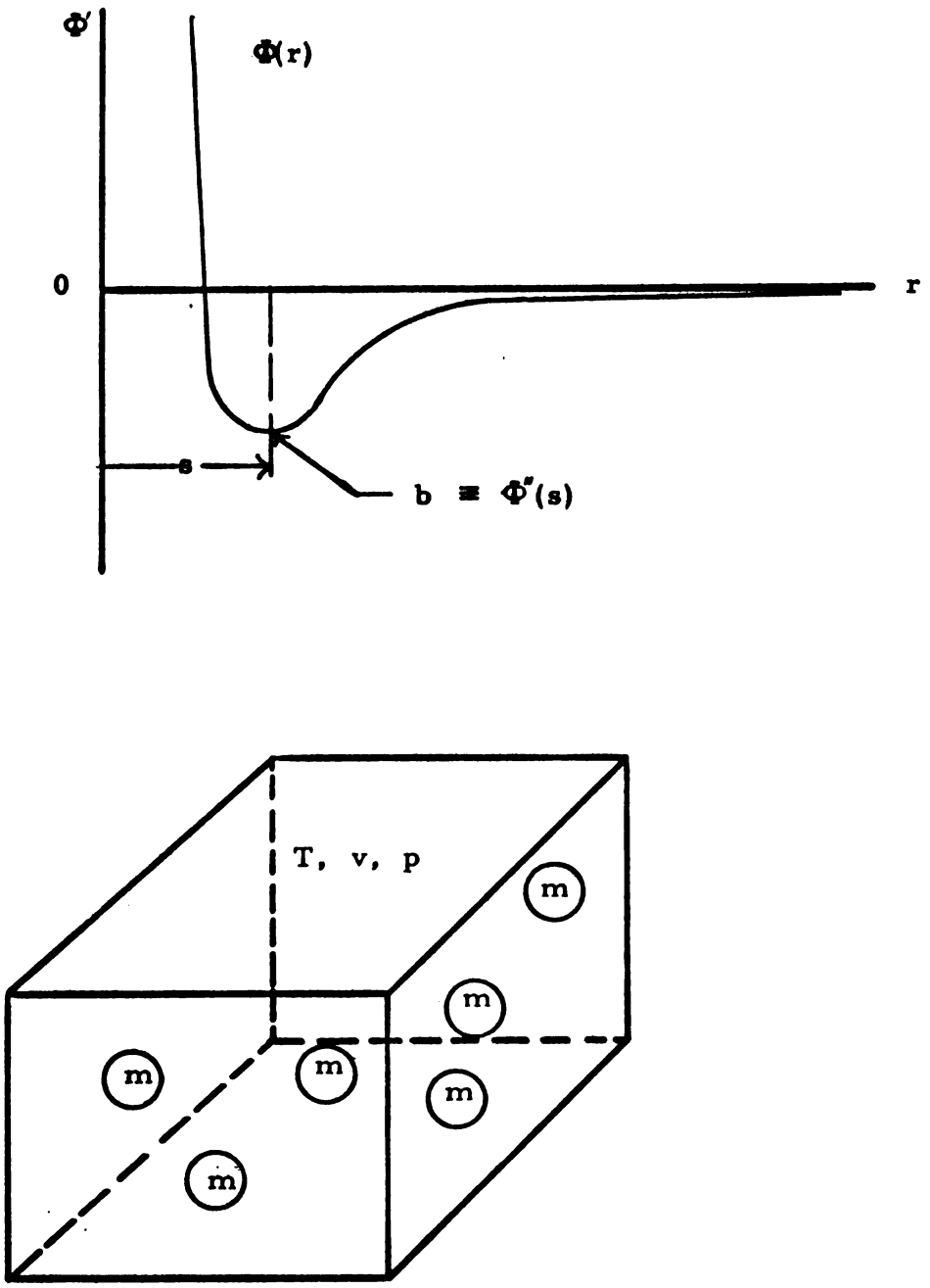

Figure 19 - Diagram to illustrate parameters relevent to dimensional analysis.

Moreover, we introduce $\hbar$ by combining it with an angular frequency $(b/m)^{\frac{1}{2}}$, to get expressly a term in the form of a quantum of energy $\hbar$ times $(b/m)^{\frac{1}{2}}$. Because there is an equation of state only two of three quantities, p, v, and T are independent, and need be included in the analysis. The seven variables to be related are: m = [mass]^1, b = [mass]^1 times [time]$^{-2}$; p = [mass]^1 [length]$^{-1}$[time]$^{-2}$ (alternatively, v = [length]^3), kT, $\hbar (b/m)^{\frac{1}{2}}$ = [mass]^1 [length]^2 [time]$^{-2}$, s = [length]^1 and η = [mass]^1 [length]^1 [time]$^{-1}$, where we have expressed each variable in terms of three fundamental units. According to the principles of dimensional analysis there exists a functional relation among 7 - 3 = 4 dimensionless products of these variables. There is some arbitrariness in the manner of expression of these variables, but for the sake of definiteness we write the relation in this form:

$$F\left[\frac{\eta s^2}{\sqrt{mkT}}, \frac{\hbar\sqrt{b/m}}{kT}, \frac{kT}{bs^2}, \frac{b}{sp}\right] = 0$$

Since we are concerned with an analysis of viscosity it is more revealing to rewrite the equation in the form

$$\eta = \frac{\sqrt{mkT}}{s^2}\,\eta^*\left[\frac{b}{sp}, \frac{kT}{bs^2}, \frac{\hbar\sqrt{b/m}}{kT}\right] \tag{6}$$

Alternatively it may be written:

$$\eta = \frac{\sqrt{mkT}}{s^2}\,\eta^{**}\left[\frac{v}{s^3}, \frac{kT}{bs^2}, \frac{\hbar\sqrt{b/m}}{kT}\right] \tag{7}$$

Here η^* and η^{**} are dimensionless functions whose detailed form can be determined only by constructing and solving the actual equations of motion for the liquid.

We can conclude immediately from equation (6) that the viscosity of separated isotopes of the same element at the same temperature and at atmospheric pressure must be proportional to $m^{\frac{1}{2}}$, apart from quantum effects. With respect to these, we can say only that at such high

temperatures that quantization energies become negligible with respect to thermal energies, the dependence of η on m must follow the square-root law. But we have no sure way of knowing how high these temperatures are. Regrettably, a technique of comparing between isotopes at "corresponding temperatures," that is, temperatures for which $h(b/m)^{\frac{1}{2}}/kT$ has the same value for each isotope, fails because of the presence of the other agument in η^* that contains T, namely, kT/bs^2. We must therefore go beyond dimensional analysis to gain further information or at least estimates of the importance of quantum effects.

As we have stated the full theoretical treatments are too complicated to permit estimating the effect of isotopic mass. Therefore we turn to the semiempirical formulas. The traditional relation, suggested in 1886 by Reynolds (15) and given explicit form by Guzman in 1913 (16), for the viscosity η, as a function of temperature T and at constant pressure p is:

$$\eta = Ae^{B/RT} \qquad \text{(Reynolds; p constant)}$$

Here A and B are supposed to be constants for a given material, but in fact are not. We have seen a typical example of the applicability of this law in the data presented earlier in this thesis. The lack of constancy is annoying but what is more serious is that the effect of isotopic mass cannot be disentangled from the quantities A and B. The effect of temperature is two-fold--the direct effect of the larger thermal energy for the individual molecules, and the indirect effect of increasing the free volume available to them. Yet this latter effect is masked in the exponential form of the equation.

Hence we seek other laws that display the dependence separately. The boldest approach is that of Batschinski (24), who argued in 1913 that the viscosity of a given substance is affected only by the increase in

free volume, regardless of the particular combination of temperature and pressure to attain it. He proposed the very simple relation

$$\eta = C/(v - b) \qquad \text{(Batschinski)}$$

where C and b are supposed to be constant, the latter being very nearly the same as the covolume occurring in the van der Waals equation for the substance. Regrettably the relation is not accurate.

To take into account both the increase in thermal energy and the increase in free volume, van der Waals Jr. in 1918 (25), proposed the relation

$$\eta = \frac{CT^{\frac{1}{2}}}{v(v-b)} e^{B/T} \qquad \text{(van der Waals Jr.)}$$

a three-constant formula that has not drawn much attention, presumably because of its complexity without a sound theoretical foundation. MacLeod in 1923 (26) suggested a generalization of Batschinski's law in modifying the form of the function containing v, but still free from the explicit dependence on T:

$$\eta = C/(v-b)^q \qquad \text{(MacLeod I)}$$

where q is a third constant. Of course, this formula can no more account for the observed variation of η with T at constant v than can the original formula. MacLeod later (1936) (27) did introduce a term containing T explicitly:

$$\eta = \frac{Ce^{B/Tv}}{(v - b)} \qquad \text{(MacLeod II)}$$

Then van Wijk and Seeder (28) in 1937 compounded the complexity by taking B in van der Waals equation not as a constant but as a function of T and v. Their theoretical foundation for the expression, however,

enabled them to show that sometimes B should be proportional to T and independent of v, whence the equation reduced to a two-constant formula.

Indeed, Brinkman (29) with this formula in 1940 was able to explain the relation between the viscosities of liquid hydrogen and liquid deuterium as observed experimentally. Here was a clear-cut case where both the masses and the moments of inertia of the molecules were in the same proportion, 2:1. The square root of this ratio is 1.4, yet the observed ratio of the viscosities was about 2.9, and nearly independent of temperature. By taking the simplified relation,

$$\eta = CT^{\frac{1}{2}}/v(v-b)$$

with $C \backsim m^{\frac{1}{2}}$, and b estimated from the observed molar volumes for liquid hydrogen and the volumes for solid hydrogen and extrapolated to $0^{\circ}K$, Brinkman was able to fit the data.

This suggests the same analysis be tried with the present data. The equation is adequate to describe the temperature dependence. The best values for both isotopes are given below:

	C	b
Li^6	2.02 mp/(cc)^2(K°)	12.93 cc/mol
Li^7	2.28 mp/(cc)^2(K°)	13.04 cc/mol

The difference in the values for b is 0.11 cc/mol, a little less than 1 part per hundred. This difference is somewhat larger than we might expect in view of the likely very small difference in atomic volume, but not significantly so. The ratio of C for the two isotopes turns out to be about 1.13, much larger than the ratio of the square root of the masses, 1.08. There seem to be no other cases in which the viscosity of two substances which have had both their moment of inertia and mass changed by the same ratio. Data for deuterated methane and

water are available (30), but it has been pointed out (31) that in these substances the moment of inertia has been changed as well as the mass. Hence any agreement here with a square root dependence would likely be fortuitous.

We may state then the following:

1) The dimensional-analysis argument advanced by Rowlinson, Pople, and others that the viscosity of isotopes of the same element at a given temperature is proportional to $m^{\frac{1}{2}}$ is incomplete. The viscosity is rather proportional to $(mkT)^{\frac{1}{2}}$, multiplied by a complementary function of $h(b/m)^{\frac{1}{2}}/kT$. In fact, in the two unequivocal instances of the examination of an isotopic substitution (that is, where the mass and the moment of inertia are changed in the same ratio), the complementary function varies more strongly with isotopic mass than does the factor $m^{\frac{1}{2}}$. (H^1, H^2: mass square root ratio, 1.4, viscosity ratio, 2.9, therefore the complementary function ratio 2.1; Li^6, Li^7: mass square root ration 1.8, viscosity ratio, 1.3, therefore the complementary function ratio 1.24.)

2. Present semi-empirical theories when simple enough to predict the effect of isotopic mass give the incorrect result.

3. Before the theories can proceed farther, many more measurements will be needed on the combined effects of temperature and pressure on viscosity, as emphasized by the experiencedtheorist, Moelwyn-Hughes (32). We submit that measurements on the effect of isotopic mass on viscosity will be at least as important, in that this effect can usually be predicted more surely than the effect of temperature or pressure, and hence may afford a critical test.

REFERENCES CITED

1. F. W. Aston, Mass Spectra and Isotopes, London: Edward Arnold, 1941.

2. E. N. da C. Andrade and E. R. Dobbs, Proc. Roy Soc., (London) A211, 12-30 (1952).

3. N. T. Ban, "The Viscosity of Molten Lithium-6 and Lithium-7," Unpublished Ph. D. dissertation, Michigan State University, 1960.

4. A. Merrington, Viscometry, London: E. Arnold, 1949.

5. G. Barr, A Monograph of Viscometry, London, Oxford University Press, 1931.

6. R. M. Lyon, Ed. Liquid Metals Handbook, Washington, D. C., U. S. Govt. Print. Office, 1954.

*7. J. E. Verschaffelt, Commun. Phys. Lab. Univ. Leyden. No. 148b, 17 (1915).

*8. R. Ladenburg, Ann. Physik, 27, 157, (1908).

9. E. N. da C. Andrade and Y. S. Chiong, Proc. Phys. Soc. (London) 48, 247, (1936).

10. Shenker, et al., Reference Tables for Thermocouples, (National Bureau of Standards circular 561, April 27, 1955), pp. 34-36.

*11. A. Bernini and C. Cantoni, Nuovo Cimento, 8, 241, (1914).

*12. L. Losana, Gazz. Chim. Ital. 65, 851 (1935).

13. D. D. Snyder and D. J. Montgomery, J. Chem. Phys. 27, 1033, (1957).

14. A. Bondi, "Theories of Viscosity," Rheology, Theory and Applications, vol. 1, ed. Frederick R. Eirich, (New York: Academic Press, 1956), 321-356.

---

*Indicates references which were not seen in the original.

*15. O. Reynolds, Phil. Trans. 177, 157 (1886).

*16. J. de Guzman, Anales de la Sociedad Espanola de Fisica y Quimica, 11, 353, (1913), 12, 432, (1914).

17. M. P. Venkatarama Iyer, Indian Journal of Physics, 5, 371-383, (1930).

18. E. N. da C. Andrade, Phil. Mag. 17, 497, and 17, 698 (1934).

19. T. P. Yao, V. Kondic, J. Inst. Metals. 81, 17 (1952).

20. E. B. Sandell, Colorimetric Determination of Traces of Metals, 2nd Ed. Interscience Publ. New York, 1950, 257-271, 362-388, 469-478.

21. J. A. Crawford, and D. J. Montgomery, Bull. Am. Phys. Soc. II, 2, 299, (1957).

22. M. F. Culpin, Proc. Phys. Soc. B70, 1069-1086, (1957).

23. P. W. Bridgman, Dimensional Analysis, Yale University Press, 1931.

*24. A. J. Batschinski, Z. Phys. Chem. 84, 643 (1913).

*25. J. D. van der Walls Jr., Proc. Ac. Amsterdam, 21, 743, 1283, (1918/19).

26. D. B. MacLeod, Trans. Faraday Soc. 19 6, 1923, 21 151, 1925.

*27. D. B. MacLeod, Trans. Faraday Soc. 32, 875, (1936).

28. W. R. van Wijk and W. A. Seeder, Physica, 4, 1073.

29. H. C. Brinkman, Physica, 7, 447, (1940).

30. J. S. Rowlinson, Physica, 19, 303 (1953).

31. J. A. Pople, Physica, 19, 668 (1953).

32. E. A. Moelwyn-Hughes, States of Matter, New York: Interscience Publishers, 1961.

---

*Indicates references which were not seen in the original.

APPENDICES

APPENDIX A

DETERMINATION OF MOMENT OF INERTIA

(Ban)

Lithium-6 Sphere	
Period	$(\text{Distance})^2$
$T_{10} = 8.795$ sec.	$d_1^2 = 5.13204$ cm^2
$T_{20} = 15.048$ sec.	$d_2^2 = 27.71601$ cm^2
$T_{30} = 12.787$ sec.	$d_3^2 = 18.18255$ cm^2

Results	
Data Used	Moment of Inertia
With d_1 and d_2	$I = 4,443.79$ gm-cm^2
With d_1 and d_3	$I = 4,443.75$ gm-cm^2
With d_2 and d_3	$I = 4,444.01$ gm-cm^2
Average value	$I = 4,443.86$ gm-cm^2

Lithium-7 Sphere	
Period	$(\text{Distance})^2$
$T_{10} = 8.821$ sec.	$d_1^2 = 5.13204$ cm^2
$T_{20} = 15.109$ sec.	$d_2^2 = 27.71601$ cm^2
$T_{30} = 12.839$ sec.	$d_3^2 = 18.18255$ cm^2

Results	
Data Used	Moment of Inertia
With d_1 and d_2	$I = 4,428.82$ gm-cm^2
With d_1 and d_3	$I = 4,424.99$ gm-cm^2
With d_2 and d_3	$I = 4,434.43$ gm-cm^2
Average value	$I = 4,429.41$ gm-cm^2

APPENDIX B

TEMPERATURE CALIBRATION

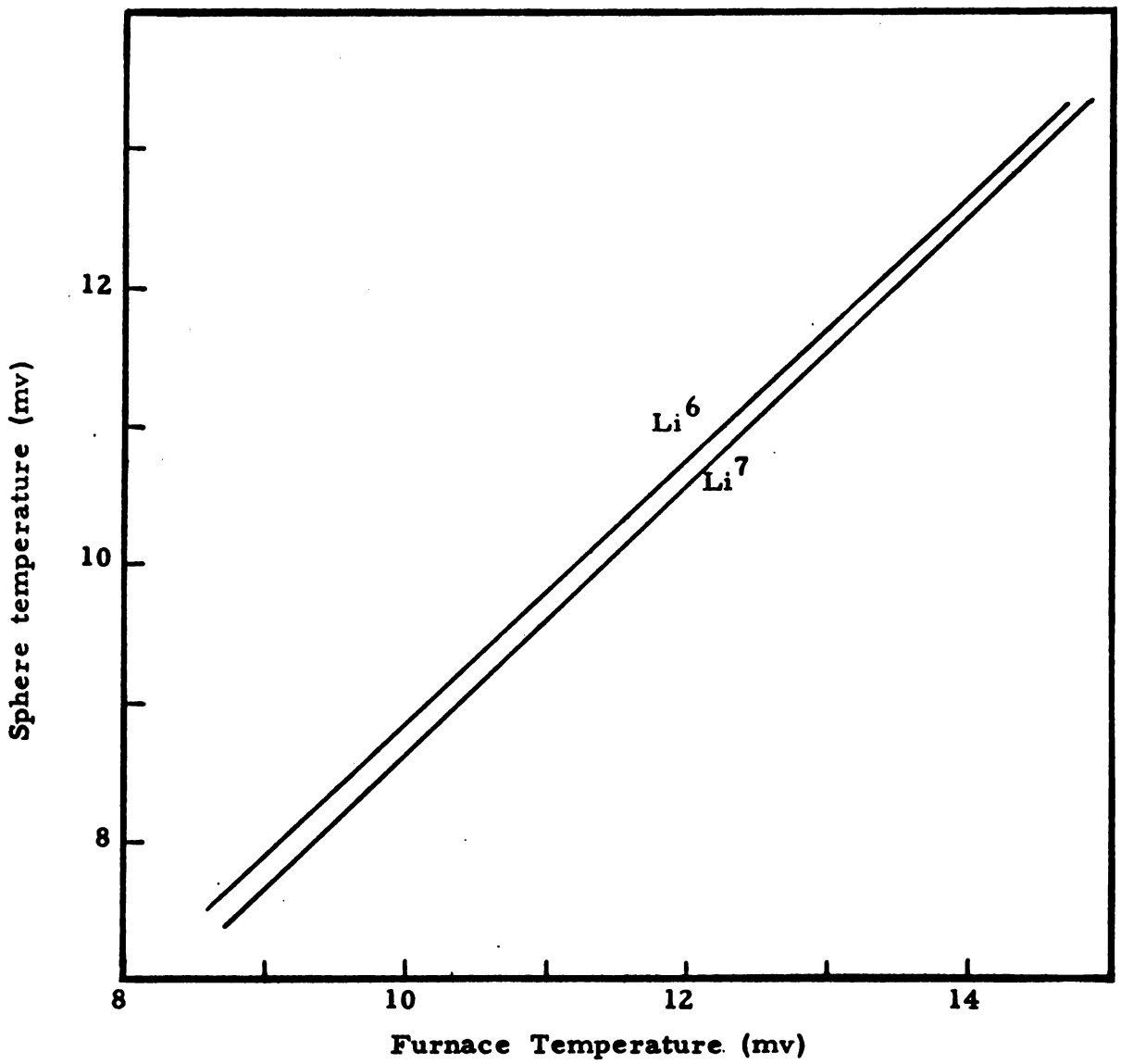

Figure 20 - Calibration relation between the sphere temperature (ordinate) and furnace temperature (abscissa).

APPENDIX C

VISCOSITY OF LITHIUM 6 DATA

(Ban)

Parameters:

Moment of Inertia	4443.86 gm-cm^2
Period (Lithium Solid)	8.795 sec.
Residual Logarithmic Decrement	40.8819 x 10^{-6}
Radius of sphere (at 20° C)	1.2827 cm
Density (At 20° C)	0.460 gm/cm^3

Sphere Temperature C°	Logarithmic Decrement x 10^6	Period sec.	Viscosity mp
188.3	482.776	8.794	4.3239
188.3	481.167	8.793	4.2768
188.3	487.582	8.794	4.4649
188.3	488.628	8.794	4.4962
188.3	485.038	8.794	4.3897
198.0	476.442	8.794	4.1533
198.0	483.129	8.793	4.3425
198.0	483.182	8.793	4.3440
198.0	481.242	8.793	4.2787
217.4	471.045	8.795	4.0231
217.4	468.990	8.794	3.9670
217.4	470.401	8.794	4.0049
217.4	470.146	8.794	3.9980
236.2	463.459	8.794	3.8374
236.2	465.757	8.794	3.8975
236.2	462.393	8.794	3.8098
236.2	462.969	8.794	3.8480
236.8	462.466	8.798	3.8144
236.8	463.749	8.798	3.8477
236.8	463.108	8.798	3.8311
266.5	456.381	8.795	3.6832
266.5	457.315	8.795	3.7067
266.5	456.848	8.795	3.6949
266.8	455.686	8.795	3.6665
266.8	456.209	8.795	3.6797
266.8	455.948	8.795	3.6731

continued

APPENDIX C - Continued

VISCOSITY OF LITHIUM 7 DATA

(Ban)

Parameters:

Moment of Inertia	4438.8928 gm-cm^2
Period (Lithium Solid)	8.7492 sec.
Residual Logarithmic Decrement	41.8851 x 10^{-6}
Radius of sphere (at 20° C)	1.2841 cm
Density (at 20° C)	0.537 gm/cm^3

Sphere Temperature °C	Logarithmic Decrement x 10^6	Period sec.	Viscosity mp
191.2	579.735	8.819	5.664
191.2	580.046	8.819	5.614
200.8	575.222	8.819	5.474
200.8	573.335	8.819	5.416
200.8	574.591	8.819	5.474
200.8	573.830	8.820	5.433
221.2	565.118	8.820	5.194
221.2	563.419	8.820	5.144
221.2	563.923	8.820	5.159
240.6	554.083	8.820	4.899
240.6	555.613	8.820	4.942
240.6	554.270	8.820	4.904
240.6	555.061	8.819	4.926
271.8	540.354	8.820	4.560
271.8	539.344	8.820	4.534
271.8	541.171	8.820	4.582
271.8	540.581	8.820	4.566

APPENDIX D

VISCOSITY OF LITHIUM 6 DATA

(Randall)

Parameters:

Moment of Inertia:	4445.1964 gm-cm^2
Period (Lithium Solid)	8.8098 sec.
Residual Logarithmic Decrement	41.0963 x 10^{-6}
Radius of sphere (at 20 C^o)	1.2828 cm.
Density (on melting)	.440803 gm/cm^3

Temperature Sphere ^oC	Furnace mv	Logarithmic Decrement x 10^6	Period sec.	Viscosity mp
180.8	9.4031	480.026	8.809	4.2251
181.8	9.4534	482.173	8.809	4.2869
182.4	9.4900	476.081	8.809	4.1165
182.7	9.5056	481.684	8.809	4.2738
183.9	9.5710	480.842	8.809	4.2509
184.6	9.6092	482.404	8.809	4.2961
185.5	9.6555	481.106	8.810	4.2608
187.9	9.7924	474.529	8.810	4.0795
188.2	9.8044	474.506	8.808	4.0773
188.3	9.8116	479.574	8.808	4.2181
188.4	9.8179	478.740	8.808	4.1947
191.3	9.9790	476.036	8.811	4.1248
191.8	10.0034	474.086	8.810	4.0707
192.1	10.0196	478.400	8.811	4.1912
192.1	10.0215	478.496	8.810	4.1930
203.3	10.6442	473.113	8.808	4.0524
203.5	10.6560	471.997	8.809	4.0232
203.9	10.6780	472.530	8.811	4.0397
204.1	10.6894	473.254	8.811	4.0596

continued

APPENDIX D - Continued

Temperature Sphere °C	Furnace mv	Logarithmic Decrement x10^6	Period sec.	Viscosity mp
221.2	11.6539	468.286	8.813	3.9424
221.2	11.6560	467.822	8.812	3.9293
221.4	11.6656	465.500	8.808	3.8651
221.6	11.6739	471.707	8.808	4.0303
221.8	11.6884	466.334	8.810	3.8889
243.1	12.9136	459.979	8.811	3.7434
243.3	12.9274	461.477	8.811	3.7818
243.5	12.9356	461.757	8.808	3.7867
265.3	14.2182	455.317	8.812	3.6453
265.5	14.2321	453.765	8.811	3.6063
267.1	14.3211	453.793	8.811	3.6082
267.1	14.3236	453.414	8.811	3.5989
287.2	15.5251	448.673	8.812	3.5005
287.7	15.5549	447.032	8.811	3.4609

APPENDIX D - Continued

VISCOSITY OF LITHIUM 7 DATA

(Randall)

Parameters:

Moment of Inertia:	4549.6853 gm-cm^2
Period (Lithium Solid)	8.9398 sec.
Residual Logarithmic Decrement	40.8761 x 10^{-6}
Radius of Sphere (at 20 C^o)	1.2841 cm
Density of Lithium (on melting)	.51458 gm/cm^3

Temperature Sphere ^oC	Furnace mv	Logarithmic Decrement x 10^6	Period sec.	Viscosity mp
181.1	9.6477	449.360	8.921	2.7461
181.3	9.6590	581.420	8.920	6.0255
184.8	9.8516	577.031	8.922	5.8815
185.6	9.8947	579.558	8.924	5.9725
186.7	9.9506	576.508	8.918	5.8606
187.1	9.9715	578.484	8.924	5.9373
187.2	9.9794	577.040	8.930	5.8962
187.2	9.9805	580.143	8.924	5.9951
187.3	9.9849	573.763	8.941	5.8000
187.3	9.9867	578.318	8.923	5.9306
187.3	9.9869	576.269	8.919	5.8548
187.5	9.9929	577.338	8.916	5.8873
187.5	9.9955	575.873	8.939	5.8692
187.6	10.0021	577.354	8.923	5.8978
187.6	10.0029	576.892	8.926	5.8862
187.7	10.0038	577.338	8.926	5.9015
187.7	10.0087	579.200	8.929	5.9702
187.8	10.0108	574.815	8.938	5.8322
187.8	10.0141	575.243	8.941	5.8510
198.3	10.5852	568.943	8.937	5.6489
198.4	10.5895	550.634	8.938	5.0788

continued

APPENDIX D - Continued

Temperature Sphere °C	Furnace mv	Logarithmic Decrement x 10^6	Period sec.	Viscosity mp
199.5	10.6495	571.214	8.920	5.7030
199.6	10.6531	571.266	8.937	5.7275
199.6	10.6550	570.513	8.940	5.7065
215.3	11.5209	559.806	8.936	5.3761
215.3	11.5234	562.031	8.939	5.4501
216.6	11.5926	559.190	8.938	5.3609
217.3	11.6320	551.695	8.940	5.1345
238.7	12.8391	550.837	8.938	5.1323
238.8	12.8434	549.985	8.938	5.1068
240.2	12.9264	550.997	8.940	5.1412
240.3	12.9321	551.557	8.941	5.1594
264.1	14.3000	540.297	8.939	4.8548
264.3	14.3134	539.236	8.936	4.8217
265.7	14.3936	538.487	8.935	4.8010
265.7	14.3955	537.335	8.939	4.7727
286.1	15.5935	530.774	8.936	4.6109
286.4	15.6117	531.051	8.936	4.6188

APPENDIX E

VISCOSITY OF WATER

Temp. °C.	η (expt.) mp.	η (std.) mp	per cent deviation
16.6	10.48	10.94	-4.2
17.1	10.42	10.80	-3.5
18.6	9.87	10.40	-5.1